Composites Part B 223 (2021) 109104

Contents lists available at ScienceDirect

Composites Part B

journal homepage: www.elsevier.com/locate/compositesb

Smart polyurethane composites for 3D or 4D printing: General-purpose use, sustainability and shape memory effect

Wendy Triadji Nugroho [a], Yu Dong [a,*], Alokesh Pramanik [a], Jinsong Leng [b], Seeram Ramakrishna [c]

[a] School of Civil and Mechanical Engineering, Curtin University, Perth, WA, 6845, Australia
[b] Centre for Composite Materials and Structures, Harbin Institute of Technology, HIT Science Park, No. 2 YiKuang Street, Harbin, 150080, PR China
[c] Department of Mechanical Engineering, National University of Singapore, Singapore, 117575, Singapore

ARTICLE INFO

Keywords:
polyurethane (PU)
3D or 4D printing
Shape memory effect (SME)
Sustainability

ABSTRACT

Excellent biocompatibility, flexibility and shape memory features of polyurethane (PU) have attracted great attention to produce various objects for particular applications in biomedical and electronic fields. The objects with complex geometry in possession of shape memory effect (SME) are arduous when being fabricated by conventional manufacturing methods such as extrusion and injection moulding so that 3D or 4D printing can be offered to overcome this drawback. Neat PU has several material demerits, especially its mechanical strength. The incorporation of the reinforcements, namely fibres, nanoparticles and other polymers, can be achieved to improve mechanical strength, shape memory capability, thermal and electrical conductivities of PU. The most interesting performance of printed structures from smart PU composites lies in a wide range of glass transition temperature allowing these innovative materials to recover to their initial shape after being deformed. Such an ability has improved the materials' usefulness, particularly for tissue scaffolds, flexible sensors and wearable devices. This review provides a holistic investigation of the current states of PU composites for 3D printing and shape memory PU (SMPU) composites for 4D printing, respectively along with their use, sustainability and SME for enormous future potential.

1. Introduction

3D printing technology commenced being developed in 1987 [1], and it then attracts researchers, governments, and industries to apply this technology to fabricate various objects based on 3D models with the aid of computer-aided design (CAD) software. This initiative is induced by several advantages based on 3D printing when compared with traditional manufacturing methods such as extrusion and injection moulding. Such a technology may manufacture a 3D structure with a complex geometry, which, however, is very difficult to be created by conventional injection moulding [2]. Besides, it is based on additive manufacturing technology that builds an object by depositing the feedstock materials layer by layer for waste reduction [3]. This characteristic contrasts with subtractive manufacturing like computer numerical control (CNC) machining, which processes a component by reducing the used material.

However, 3D printing cannot entirely replace traditional manufacturing because it has several issues related to printing speed, surface finish and mechanical properties of printed parts. The fabrication process of this technology is relatively slow as opposed to extrusion and injection moulding, and thus it may not be suitable for large-scale production [4]. The printed parts produced by 3D printing typically possess a rough surface caused by staircase effect [5]. Concerning this, Nanyang Technological University has developed the stepless rapid prototyping (SRP) [6], which is implemented to the 3D printing setup in order to reduce staircase effect, as well as to improve surface finish and dimensional accuracy of printed parts.

3D printing involving time, stimuli, programming and smart materials can be further transformed into 4D printing [7]. The term time here does not correlate with the manufacturing time of parts. Instead, it indicates that the printed parts continue to change over time after the manufacturing process [8] and further recover their original shape when subjected to external stimuli such as heat, applied loads, light, pH level, evaporation, magnetic and electrical fields [9]. This viewpoint has been supported by Pei [10] mentioning that conventional 3D printing enables to produce a static object. Whereas 4D printing combines carefully

* Corresponding author.
E-mail address: Y.Dong@curtin.edu.au (Y. Dong).

https://doi.org/10.1016/j.compositesb.2021.109104
Received 4 March 2021; Received in revised form 20 June 2021; Accepted 22 June 2021
Available online 24 June 2021

designed geometries with accurately controlled deposition of active (smart) materials inducing shape change under external stimuli. The term *programming* refers to the shape-setting of printed parts, in which the 3D printed part enables to be deformed by an external force under a particular external stimulus (e.g. heat, light, magnetic and electrical fields) [7,8]. The basic concept of 3D or 4D printing is presented in Fig. 1.

One of popular raw materials used as the feedstock material for 3D printing is polyurethane (PU). This material belongs to a family of polymers created through the reaction of diisocyanate, oligodiol (i.e. polyol or macrodiol) and a chain extender (diamine or diol) [11,12]. Oligodiol forms the soft segments while the isocyanate and the chain extender build the hard segments. The separation between soft and hard segments, known as microphase separation, produces the elasticity to PU. Besides, it also determines PU properties such as mechanical property, hydrolytic resistance and thermal stability [13,14]. The modification of these segments results in the variation of tensile and elastic properties of this material.

Polyurethanes (PUs) are available in several different forms (i.e. thermoplastics, thermosets, foams, elastomers and fibres) [15]. In particular, thermoplastics and thermosets can exhibit SME, which is well known as shape memory polyurethane (SMPU). The primary difference between SMPU and conventional PU lies in their various ranges of glass transition temperature (T_g). SMPU possesses a wider range of T_g so that when this material is cooled from above to below T_g under a mechanical load, the material shape is deformed. Additionally, this load is locked into the polymer even though it has been removed. By implementing an external stimulus, namely heating above T_g, this material may recover its initial shape.

Both PU and SMPU have excellent flexibility and biocompatibility to meet specific requirements of tissue engineering as biodegradable scaffolds [14,16–22]. However, they also have typical drawbacks such as weak thermal stability and slow reaction rate. Concerning this, a new approach has been introduced to create phenolic resin/PU copolymers by incorporating oxazine and urethane groups in one molecule. This approach has been successful in improving thermal stability and tensile strength of such copolymers [23]. Besides, it is also worth mentioning that the use of isocyanates in PU production entangles hazardous and toxic phosgene, and the manufacturing process of these monomers involves safety devices and enormous investments. Non-isocyanate polyurethanes (NIPUs), when derived from five-membered cyclic carbonates produced via a simple reaction between epoxides and carbon dioxides, may be offered to yield PU by meeting the requirements related to the environmentally benign and safe processes [24].

The work concerning PU and SMPU has been available in many different studies mentioned previously [25–28]. However, the number of review articles that focus on using these materials for 3D or 4D printing along with their sustainability is still rarely seen. Moreover, a comprehensive discussion related to some extraordinary properties of PU and SMPU composites such as biocompatibility and flexibility is required by medical world to produce tissue scaffolds, flexible sensors, actuators and wearable devices in order to help people with disabilities or amputation on their body organs like hands and legs due to accidents.

This paper aims to fulfil those requirements and mainly concentrate on the current state and future trends of PU composites for 3D printing and SMPU composites for 4D printing accordingly. Besides, it also discusses the sustainability of PU for 3D printing, mixing methods to produce the feedstock materials for 3D printing and the properties of printed parts. This review starts with the characteristics of PU and the concepts of 3D or 4D printing. An overview with respect to PU composites for 3D printing and SMPU composites for 4D printing is further elaborated. It is then followed by feeding stock material preparation for 3D or 4D printing consisting of purification, dehumidification and mixing processes. The sophisticated processes of 3D printing of PU composites and 4D printing of SMPU composites, involving composite micromechanics concepts in the microstructures and properties of the printed parts, are exclusively covered. Finally, the applications of 3D or 4D printing of PU and SMPU composites are detailed along with the summary, challenges, and future trends applied in 3D or 4D printing of PU composites.

2. General-purpose, biodegradable and sustainable polyurethane (PU)

PU is one of such essential polymers possessing unique properties ranging from liquid, soft, and rubbery solids to rigid thermosets and thermoplastics. These properties are fundamental aspects relating to shape memory properties. PU has been widely implemented in various applications including structural foams [29,30], coatings [31,32], adhesive [33], fibres [34] and biomaterials [35,36] owing to its remarkable abrasive resistance, low-temperature flexibility, high toughness, excellent corrosive resistance and a wide range of available mechanical strengths [37].

2.1. General-purpose polyurethane (PU)

The first PU, called Perlon U, was made from 1,6-diisocyanatohexane and 1,4-butanediol (BDO) by Professor Otto Bayer in 1937, who was well recognised as the "father" of PU industries [38]. This work was focused on the fabrication of fibres and flexible foams with excellent properties. PUs based on 1,5-diisocyanate and polyester resin were utilised to reinforce the military aircrafts in order to enhance their

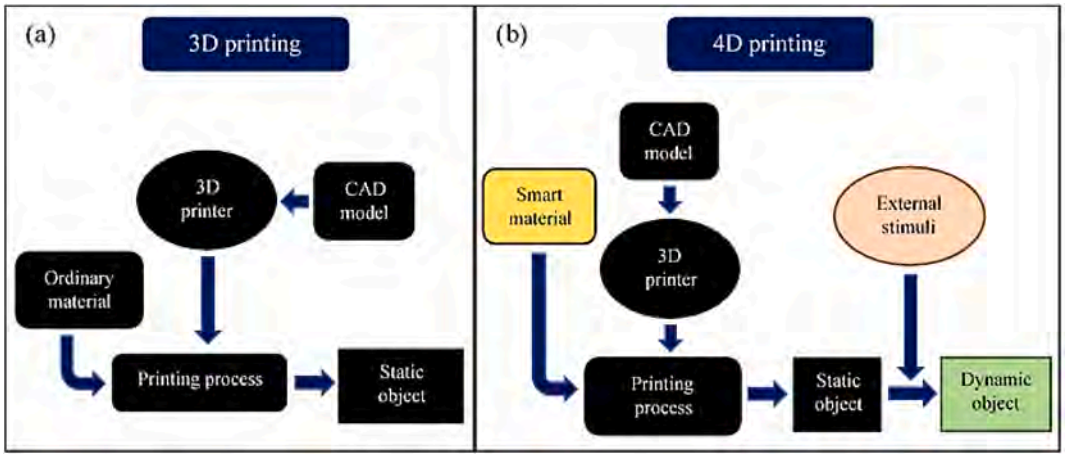

Fig. 1. Basic concept of (a) 3D printing and (b) 4D printing.

strength and performance. The PU products were commercially available and initially developed very fast in the 1950s. These products were typically used as foamed materials as well as elastomers, and their commercial applications have grown dramatically over the past 70 years [34].

PU is formed through a reaction between isocyanate functional groups (NCO) and hydroxyl (OH) groups of polyols. The name of this material is associated with the resulting urethane linkage [39]. The forming reaction of PU is exothermic where this reaction releases the energy via heat or light, as illustrated in Fig. 2. In this chemical reaction formula, isocyanate and polyol groups, which are written as R_{iso} and R_{polyol}, are derived from isocyanate monomers and polymer components, respectively. To achieve sufficient elasticity, soft polyols typically have a molecular weight ranging from 400 to 6000 g mol^{-1} while hard segments (i.e., diisocyanate and chain extender) contain less than 50 wt% [40]. However, another study revealed that with a much higher molecular weight of 32,000 g mol^{-1} for poly (dimethyl siloxane) (PDMS) of soft segment oligomers and 2–5% hard segments, such a composition yielded excellent elastomeric property (i.e. 300-600% strain at break) [40]. It could be induced by the remarkable improvement in phase separation between hard and soft segments of PDMS PUs/polyureas and the chain entanglement of PDMS. Four different forms of PUs, namely thermoplastics elastomers, thermosets, foams and fibres along with their general-purpose use, are further discussed to provide the fundamental knowledge of such materials.

Thermoplastic polyurethane (TPU) elastomer is one of popular PUs consisting of soft and hard segments in an alternating manner (Fig. 3). The soft segments with a low glass transition temperature (T_g) build the continuous matrix for low-temperature flexibility. Whereas the hard segments in possession of relatively high T_g tend to self-assemble into domains via crosslinks. These domains commonly become reinforcing fillers in the continuous matrix with a low T_g and enhance the material properties such as mechanical strength, solvent resistance and thermal performance [34]. The physical crosslinks are typically reversible in nature, which means that above T_g, both soft and hard segments appear to be soft in the formation of a homogeneous mixture. This unique characteristic is generally attributed to its morphological structures created by corresponding particular chemical structures and processing conditions. Hence, it is crucial to understand the structure-property relationship of TPU to further develop this material along with the future potential to biomedical and electrical applications.

Thermoset PU is derived from a soft solid or thick liquid prepolymer or resin. This resin is changed into an insoluble polymer network through a curing process induced by heat or by mixing with a catalyst. Dissimilar to TPU that can be melted, thermoset PU does not soften or melt when heated. However, it also consists of two major parts, which are known as soft and hard segments. Soft segments are made up of polyol while the hard segments comprise reacted diisocyanate and chain extender [41]. When compared with TPU, thermoset PU possesses better heat and abrasive resistance, higher hardness and ability to hold a higher load. Nevertheless, it is less durable than TPU, and cannot be reformed, which may restrict its widespread applications in manufacturing industries. The great efforts have been made to overcome this drawback, such as the development of thermoset PU composites to yield better durability and elasticity.

PU foam can be found almost everywhere because of its broad applications in many areas of electronics, building and biomedical engineering, etc. This material possesses better properties than other

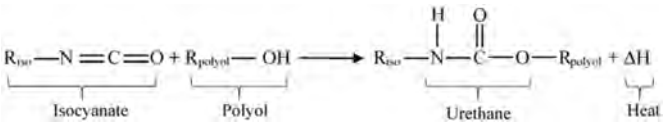

Fig. 2. Chemical reaction of urethane production.

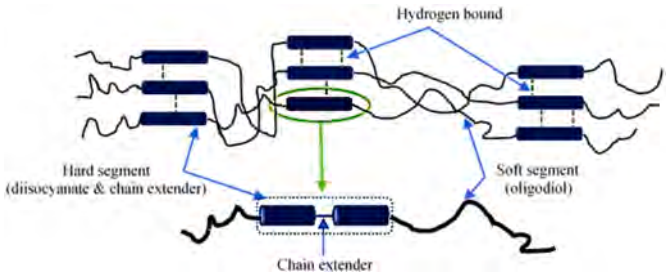

Fig. 3. Chemical structure of TPU.

polymeric foams, as exemplified by low density and thermal conductivity. Such properties make PU foam a suitable material candidate for thermal and insulating applications [42]. The growing interests in electronics like computation, communication and automation have enhanced the electromagnetic interference (EMI) leading to pollution. PU foam composites used as EMI shielding successfully reduced this pollution level [43]. Besides, this material also possesses an excellent sound absorption property in order to meet the building requirements especially for theatres, sound studios and offices [44]. Even though this material offers many advantages, several limitations are still worth mentioning. For instance, the biostability of PU foam becomes a typical issue due to its instability in water and oxygen environments. Nevertheless, this problem may be overcome with the use of polysiloxanes and polyolefins [45]. Another drawback lies in high dependence on petroleum for the production of PU foam with the compliance of strict regulations. As such, renewable raw materials and improved manufacturing technologies like 3D printing could be a viable solution to tackling such a problem.

PU fibres are considered as synthetic fibres made from a long-chain synthetic polymer with the inclusion of at least 85% segmented PU [46]. A unique property that differentiates this material from other human-made fibres is a combination of a high degree of an extension, which is followed with its ability to restore its original length quickly. PU fibre is similar to rubber with several advantages such as better strength, higher resistance to abrasion, bending and aging, lower density and better dyeability. Besides, it also has a large modulus and a high degree of highly elastic restoration to allow for the creation of fabrics with a large form-stability [47]. These characteristics are crucial in the use of textile articles. Therefore, this material is utilised to fabricate sporting clothing (e.g. ski suits and swimsuits), orthopedic hosiery and objects of feminine clothing. However, PU fibres are quite sensitive to high temperature. Even though it is resistant to the action of organic acids or dilute mineral at normal temperature, it can degrade to a greater or less extent upon heating [47]. The progress in the processing of synthetic fibres is anticipated to accelerate the development of new fabrics and technical articles by implementing unique characteristics of PU fibres.

2.2. *Biodegradable and sustainable PU*

Biodegradable polymers that are chemically synthesised like PU offer numerous advantages as opposed to natural macromolecules in relation to their processing, applications, and industrialisation. Besides, mechanical, physicochemical, and functional properties, as well as biodegradability of these materials may be precisely tailored by changing the synthetic strategies and conditions in order to meet specific application requirements [48].

Biodegradability of the material is necessary for specific applications such as biomedical engineering due to its connection with living organisms like human and animal bodies. For instance, raw materials used for tissue engineering and drug release systems [49] should degrade in physiological environments at a particular time after those materials have accomplished their tasks. Otherwise, they must be ejected from the

body to prevent any adverse effects (e.g. infection, poisoning or injuring internal organs) that may harm human or animal lives. The in vivo degradation rate of PU is primarily governed by the hydrolysis of ester groups leading to degradation products of α-hydroxy acids [50]. The hydrolysis of urethane groups in hard segments produces urethane and urea fragments with terminal acid groups, which occurs at a slow rate, and the concentration of acidic degradation products may cause autocatalysed degradation, as well as adverse tissue reaction [51]. Overall, the chemistry of biodegradable PU should be optimised to meet the requirements in terms of biocompatibility, nontoxicity of absorbable degradation products, drug release profile and tissue-mimicking mechanical properties [49].

The term "sustainable" in this review refers to renewable raw materials for producing PU to replace conventional petroleum-based materials. Three fundamental reasons spark the replacement action. First of all, the quantity of oil decreases year by year due to a significant increase in fuel consumption. Secondly, such a material causes environmental damage while the application of Green Chemistry principles is highly recommended instead [52]. The governments are urged in many countries to impose stricter regulations relating to the use of petroleum-based raw materials. The last reason is the number of renewable materials such as lignocellulosic biomass and vegetable oils [53] are abundantly available in nature.

However, the replacement of non-sustainable materials (i.e. petroleum-based isocyanates) still becomes quite challenging till now. Therefore, most research is dedicated to developing PUs with increasing the renewable content with the consideration of using polysaccharides, lignocellulosic biomass and natural oils as polyol sources. Lignocellulose possesses non-editable property and significant hydroxyl functionality. In particular, it has many quantities in nature where these advantages promote this material as a renewable means for PU fabrication [54]. Such a material comprises cellulose, hemicellulose and lignin as the primary compounds among other elements (e.g., tannins, protein and ash) despite unequally distributed composition, as well as strong dependence on the biomass property [55]. Lignin possesses the reactive and hydroxyl-groups characteristics, and it is obtained as a by-product in paper and pulp industries. It makes this material appropriate as a potential precursor for PU production [56]. Lignocellulosic biomass should be modified to improve the accessibility of hydroxyl groups for steric hindrance, and then it further reacts with isocyanate moieties [57]. The excellent properties of vegetable oils such as sustainability, non-toxicity, easy handling, structural versatility and abundant availability become a driving force of their feasibility as polyol sources [48]. Their potential can meet the requirements of sustainable development standards as feasible alternatives to replacing unsustainable raw petroleum-based materials in order to produce renewable and cost-effective PUs [47]. The presence of amenable unsaturation and ester groups in vegetable oils provides excellent chemical versatility [51] so that it makes them a reasonable chemical means for sustainable PU development.

3. PU composites for 3D printing

Neat polyurethane (PU) offers a great elongation of approximately 400%, but it possesses low mechanical strength. Therefore, the reinforcement materials such as fibres and particles are utilised to improve its mechanical strength. The addition of reinforcements in the PU matrix yields PU composites which are required to make 3D structures, namely scaffolds, flexible sensors and wearable devices. Some of those structures are arduous to be made by the conventional techniques, such as extrusion and injection moulding in possession of complex geometries and voids [2]. Therefore, a new manufacturing technology is desired to allow for the fabrication of such structures. 3D printing with its unique rapid prototyping characteristics can accomplish this specific task and may further reduce waste materials thanks to the built-up structures in a layer-by-layer manner [3].

Some of the 3D printing techniques used to process PU and PU composites are fused deposition modelling (FDM), selective laser sintering (SLS), direct ink writing (DIW) and digital light processing (DLP). FDM is a very popular method among all 3D printing techniques since it can process various raw materials, which are inexpensive and user-friendly [26]. The advantage of SLS lies in no required support material when building a structure resulting in the cost reduction of materials. Besides, SLS produces a part with higher accuracy and better surface finish as opposed to FDM [2]. DIW allows incorporating bioactive materials, namely a growth factor, in the feedstock to enhance the printed scaffold functionality [17]. Therefore, DIW is employed more frequent in biomedical applications. In general, DLP can yield the highest accuracy and surface finish compared to FDM, SLS, and DIW. It fabricates the 3D objects based on the photopolymerisation process, which uses a light projector to project images onto the polymer surface [2,25]. It means that DLP could become the best option when the printed parts are required to yield high accuracy and surface finish obtained from UV-curable resins. Such four techniques, consisting of FDM, SLS, DIW and DLP, have unique characteristics that can be applied to create a printed part from both PU and PU composites. A summary of PU and PU composites used for 3D printing is presented in Table 1.

The form of PU used in 3D printing can be pellets, powders, filaments, or even in liquid form. FDM typically handles TPU in the solid form (i.e., pellets, powders and filaments) according to its processing characteristics based on the extrusion method. In this method, PU and its composites must be mixed first in a filament extruder to produce a composite filament with common diameter sizes of 1.75 or 2.85 mm [58,59,66]. Such filaments are then employed as the feedstock materials for FDM to build 3D objects.

PU used for SLS technique should be in the solid form (e.g. powders) since this technique is based on the powder bed fusion (PBF) technology that applies a laser as the heat source to sinter powdered materials for the fabrication of PU composite structures [72]. In this fabrication process, the laser movement is directed by machine controller with reference to 3D models created using CAD software.

In DIW printing, PU and its composites should be synthesised in order to become the feedstock material for this technique. The primary requirement of this feedstock material in ink form is the sufficient ink viscosity. The properties of ink such as viscosity must warrant this ink can be extruded via a syringe tip and deposited layer by layer onto the building substrate [73]. Once the ink exits from a syringe tip, it should solidify rapidly to maintain its structure. Otherwise, the structure may damage due to the prior layer has not entirely solidified yet when loaded by the new layer.

UV-curable PU resin is used as the feedstock material in DLP since this technique works based on a photopolymerisation process and applies UV light to cure that resin for the production of 3D components [74]. Fillers or reinforcement materials may be added in UV- curable PU resin to improve the properties of printed parts though it must not reduce the curable ability of that resin. One primary challenge for photopolymers to be used for DLP technique is associated with their viscosity [75]. Photopolymers with too high viscosity give rise to longer print time as the best scenario [4], or warpage of printed components as the worst scenario [76]. Therefore, the optimum viscosity value is required to be obtained so that printed parts can be yielded with high accuracy and good surface finish.

3.1. Preparation of PU composites for 3D printing

The preparation of PU composites for 3D and 4D printing typically consists of three processes: purification, dehumidification and mixing. Purification can be interpreted as a separation of a particular component from a mixture [77] while dehumidification refers to the decreased moisture content in the material and mixing aims to combine some elements into one mass typically based on constituent blending.

Table 1
Summary of PU material and its composites for 3D printing.

PU			Composites			3D printing technique	Ref.
Type	Specification	Supplier	Type	Specification	Supplier		
TPU	• Pellet • Elastollan 1185A grade of TPU polymer • Density: 1.12 g cm^{-3} • Shore hardness: 85A	BASF	Multi-walled carbon nanotubes (MWCNTs)	NC7000 and long MWCNTs	Nanocyl S.A. (Sambreville, Belgium)	FDM	[58]
TPU	• Pellet • Pearlthane 11H94 • Specific gravity: 1.18 g cm^{-3} • Hardness: 95 (shore D) • Tensile strength: 42 MPa	Lubrizol	Cork	• Powder • Granulometry inferior to 0,25 mm • Thermal conductivity: 0.045 W m^{-1} K^{-1} • Density: 120–240 kg m^{-3} • Thermal diffusivity: 1 $\times$ 10^{-6} m^2 s^{-1}	Corticeira Amorim	FDM	[59]
TPU	• Pellet • Elastollan 1185A • Density: 1.12 g cm^{-3} • Shore hardness: 85A	BASF	MWCNTs	• Powder • Nanocyl - NC7000 90% purity • Average diameter: 9.5 nm • Average length: 1.5 μm	Nanocyl SA	FDM	[26]
TPU	Filament	Saintsmart	Polylactic acid (PLA)	Filament	Saintsmart	FDM	[60]
TPU polyester elastomer	• Powder • Semiflex with shore hardness of 95A • Filament diameter: 1.75 mm	NinjaTek, Manheim, PA, USA	Zeolitic imidazolate framework (ZIF)	ZIF-8 powder (Basolite Z1200)	Sigma- Aldrich (St. Louis, MO, USA)	FDM	[61]
TPU	• Powder • Bayer 2195 • Melt flow index: 12.1 g/10 min • Density: 1.19 g cm^{-3}	Bayer Co. Ltd	MWCNTs	• Powder • NC7000 • Length: 1.5 μm • Diameter: 9.5 nm	Nanocyl SA (Belgium)	FDM	[62]
TPU	• Elastollan TPU C95A • Density: 1.24 g cm^{-3} • Tensile stress: 50 MPa • Elongation: 550% • Hardness: 95A • Melting temperature: 200°C	Deansheng Plastic Company, Harbin, China	Wood flour (WF)	Size: 150 μm (100 mesh)	Lingshou County Mineral Processing Plant, Harbin, China	FDM	[63]
TPU	HF-4190A	Huafon TPU Co., Ltd.	Hexagonal boron nitride (hBN)	• Platelet • PN08 • Average particle size: 8 μm	Zibo Jonye Ceramics Technology Co., LTD	FDM	[64]
TPU	Shore hardness: 95A	ESTANE,W ickliffe, OH, USA	MWCNTs	• Purity content: 90% • Diameter in the range of 8–15 μm	Kumho Petrochemical Co., Ltd., Seoul, Korea	FDM	[65]
TPU	• Pellet • TPU 5377, with a density of 1.14 g cm^{-3} • Elongation at break: over 700%	Bayer Company, Germany	PLA microfibres	• Pellet • PLA 4032D • Density: 1.24 g cm^{-3} • Melt flow index: 7 g/10 min (210 °C, 2.16 kg)	Nature Works, USA	FDM	[66]
TPU	• TPU powder (Bayer 2195) • Melt flow Index: 17.5 g/10 min (215 °C, at a pressure of 10 kg) • Density: 1.12 g cm^{-3}	Bayer Co. Ltd	• MWCNTs • Silver nanoparticle (AgNP)	• MWCNT NC7000 • Average length:1.5 μm • Nominal diameter: 9.5 nm • 97% purity	• Nanocyl SA (Belgium) • Chengdu Kelong Chemical Reagent co. Ltd	FDM	[67]
Poly(ε- polycaprolactone) (PCl diol) Polyethylene butylene adipate (PEBA) diol	• M_n : 2000 Da • M_n : 2000 Da	• Sigma, USA • Greco, Taiwan	• Isophorone diisocyanate (IPDI) • 2,2-bis(hydroxy methyl) propionic acid (DMPA) • Ethylenediamine (EDA)		• Evonik Degussa GmbH, Germany • Sigma, USA • Tedia, USA	Direct ink writing (DIW)	[17]

(*continued on next page*)

Table 1 (*continued*)

PU			Composites			3D printing technique	Ref.
Type	Specification	Supplier	Type	Specification	Supplier		
TPU	• Powder • Luvosint X92A-1	Luvocom, Germany	CNTs	• NC7000 • The average diameter: 10–15 nm • The average length: 1.5 μm	Nanocyl, Belgium	Selective laser sintering (SLS)	[68]
TPU	Powder	Nanjing Mophene 3D Technology Co., Ltd., China	Single-walled carbon nanotubes (SWCNTs)	• SWCNTs TUBALL™ material • Mean Diameter: 1.6 ± 0.6 nm • Length: > 5 μm	OCSiAl	SLS	[69]
UV-curable PU resin	Possessing a composition as follow: 45–47 wt% polyurethane acrylate, 34–36 wt% morpholine, and 15–17 wt% tripropylene glycol diacrylate	Wanhao Precision Casting Co. Ltd. (Jinhua, China)	Oil palm empty fruit bunch (EFB) fibres		Szetech Engineering Sdn Bhd (Selangor, Malaysia)	Digital light processing (DLP)-stereolithography (SLA)	[25]
PU resin solution	Carima Acryl, CFY063W	Carima (Seoul, Korea)	• Polyaniline (PANI) • Graphene sheet (GS)	• Aniline (99%) • Density: 25 mg mL^{-1} • The average thickness: < 5 nm • The size: 2–3 μm	• Sigma– Aldrich (St. Louis, MO, USA) • MExplorer Co., Ltd. (Ansan, Korea)	DLP-SLA	[70]
Photo- curable PU	Possessing a composition as follows: 45–47 wt% polyurethane acrylate, 34–36 wt% morpholine, and 15–17 wt% tripropylene glycol diacrylate	Wanhao Precision Casting Co. Ltd. (Jinhua, China)	• Oil palm empty fruit bunch (EFB) fibres • Graphene nanoplatelet (GNP)		• Szetech Engineering Sdn Bhd (Selangor, Malaysia) • Sigma Aldrich, Darmstadt, Germany	DLP-SLA	[71]
UV-curable PU resin	• PLA-PUA oligomer (polylactic acid– polyurethane, made from acrylate- modified polylactide diol with a purity of 99% and Mw: 2000–30000	Shenzhen Esun Industrial Co. Ltd	• Trimethylolpropane trimethacrylate (TEGDMA) • Phenylbis (2, 4, 6-trimethylbenzoyl)-phosphine oxide (Irgacure 819) • Graphene	• Irgacure 819, green powder • 1–2 μm in length and 2–5 nm in thickness	• Sumda Material Technology Co. Ltd • BASF Co. Ltd • Allightec Co. Ltd.	DLP-SLA	[18]

3.1.1. Purification and dehumidification process

PU composites for 3D printing must be dried and sieved to reduce their moisture content and remove their impurities according to Li et al. [68]. This study used TPU, CNTs and polyamide 12 (PA12) powders as raw materials according to SLS technique to fabricate the printed composites. In the preparation of TPU/CNT powders, a Buchner funnel was employed to filter TPU/CNT mixture suspension under reduced pressure. Dehumidification, which is known as a drying process, was conducted in a vacuum oven at 50°C for 24 h to lower the moisture content of TPU/CNT powders. These powders were then sieved to eliminate particles with undesirable sizes [68]. This work implemented two purification methods including filtration and sieving, as well as one dehumidification technique as a drying process. The drying and sieving methods were also used by Gan et al. [69] to prepare TPU/SWCNT nanocomposites in powder form for SLS printing.

Other techniques such as evaporation, washing and drying can be utilised to purify and lower the moisture content of PU composites. Ibrahim et al. [71] employed a vacuum filter and evaporator to remove the pulp from the organosolv lignin and separate the organosolv solution from the extracted lignin in the lignin extraction process. This organosolv solution underwent an evaporation process until the solvent was entirely removed. The excess formic acid was eliminated from the lignin using repeated washing, and then this lignin was recovered via an oven-drying process.

3.1.2. Mixing process

Two materials or more with different physical or chemical properties that are mixed or combined will form a composite. The mixing method affects the filler distribution in the matric in order to enhance the composite properties such as mechanical strength, Young's modulus, thermal and electrical conductivities. Additive manufacturing or known as 3D printing fabricates a structure layer by layer [78]. Structures produced by this technology may be considered as laminate-like mesostructures, formed as printed paths that are partially bonded and fused together. It means that the mixing method has a direct impact on the properties of printed parts. Therefore, the mixing method should be carefully selected to yield the printed composites with desired properties, geometries and surface finishes.

This review partly focuses on PU composites for 3D printing where PU acts as the matrix, while other materials such as different polymers, fibres, and nanoparticles can become the fillers or reinforcements. To combine constituent materials to be a composite requires a mixing process to be adapted with the nature of those materials. Accordingly, three types of mixing methods consisting of solution mixing, melt mixing, as well as a combination of solution and melt mixing are discussed in this paper.

Solution mixing typically is used to prepare PU composites for 3D printing techniques such as direct ink writing (DIW), selective laser sintering (SLS) and stereolithography (SLA) [69,71,79]. Eom and Won [79] utilised solution mixing to mix PU resin and other materials to form PU composite for DIW printing. In this work, PU resin was mixed with urea-formaldehyde resin (UF), acetone, formaldehyde, and water to form the shell material while polyolefin-based structural fibre was used as the core. Shell materials were deposited onto the core material surface by using DIW technique to create composite structures. This coating was aimed to protect core materials, thus improve bonding behaviour between the fibres and cement matrix, as well as render the hydrophilicity to fibre surfaces. Solution mixing was also employed by Gan et al. [69] to blend TPU and single-walled carbon nanotubes (SWCNTs) to produce composite powders for SLS printing. At first, SWCNTs were pre-dispersed using a wet ball milling process, and then they were mixed with polyvinylpyrrolidone (PVP). This mixture was rotated at a low speed of 300 rpm to prevent the shear stress in order to break up SWCNTs. The dispersion obtained was transferred to a beaker with the addition of anhydrous ethanol. Ultrasonication was conducted to achieve stable SWCNT dispersion, to which TPU powders were then added with a continued mechanical stirring for 2 h [69].

The fabrication of feedstock materials for SLA printing, derived from combined renewable materials (i.e. natural lignin), GNPs and photocurable PU, involves the solution mixing. Lignin is extracted from oil palm empty fruit bunch (EFB) fibres through an organosolv process. This lignin was mixed with GNPs using a homogeniser for 30 min, and photocurable PU was then added to this solution. The whole process took place for 10 min until the particles were homogenously dispersed [71]. Su et al. [80] applied solution mixing to blend PU paint with carboxymethyl cellulose (CMC) or silicon oxide (SiO_2) nanoparticles in order to create PU paint-based composites for 4D printing. The addition of CMC or SiO_2 particles to the PU paint was followed by a stirring process to yield the viscoelastic composite paste for modified FDM. It was deemed as a modified FDM since original extrusion nozzle was replaced by a digital syringe dispenser so that this technique looked like DIW printing [80]. This study offered a simple and inexpensive method to induce SME in 4D painting. However, the use of this method is still limited to the painting field only. It is anticipated in the next few years that this technology can be applied as the warning signs in engineering equipment under the stimuli of heat.

The melt mixing method uses high-shear extruders or mixers to blend raw materials. It takes place above T_g or the melting point of polymers, which is typically utilised in FDM. The matrix and reinforcements applied in this method are common thermoplastics or elastomers and nanoparticles or chopped materials [61,62]. Important equipment required in melt mixing is a filament extruder. The extruder used in 3D printing for PU composites is typically divided into two types, namely single-screw extruder and twin-screw extruder. The superiorities and drawbacks of both types are presented in Table 2.

It is generally understood that a single-screw extruder suits filament production with small outputs, medium filament quality and low-cost investment. Otherwise, twin-screw extruder becomes the better choice particularly for good dispersion of particles/fibres in composite materials.

Melt mixing method has been employed by Tzounis et al. [58] to fabricate the filaments from TPU and MWCNTs used for the feedstock material in FDM. This study relied on a small-scale twin-screw extruder

Table 2
Pros and cons of single and twin-screw filament extruders.

Parameter	Single-screw extruder	Twin-screw extruder
Capital cost	low	high
Heat of friction	high	low
Usage procedure	easy	more complicated
Compounding ability	low	high
Assemble and disassemble	easy	difficult
Energy consumption	low	high
Stay time	long	short
Rotary speed	low	high
Conveying efficiency	low	high
Versatility	low	high
Process productivity	low	high

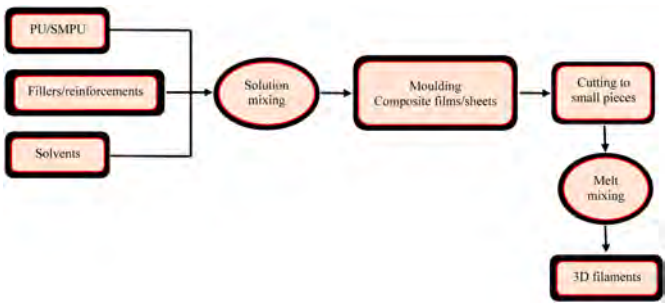

Fig. 4. The combination of solution and melt mixing process.

to perform a melt mixing process by applying extruding parameters such as melting temperature of 219–228°C, screw rotational speed of 300 rpm and screw length-to- diameter (*L/D*) ratio of 36, respectively. Similarly, Leng et al. [66] and Jing et al. [20] also used a twin-screw extruder to mix raw materials consisting of TPU and PLA. The primary distinction was that the former took an ordinary TPU as the matrix material and employed a twin-screw extruder to prepared composites in a granular form. These composite granules were then further melt-extruded by a single-screw extruder to create the filaments for FDM technique. Whereas the latter selected SMPU, blended with PLA to produce composite structures and identify their shape memory features. A single-screw extruder was utilised to perform a melt mixing process in order to yield the 3D filaments originating from TPU and cork [59]. At first, TPU pellets should be milled and sieved to produce TPU powders. These powders were then blended with cork powders and dried in an oven to reduce the mixture moisture content. In the following process, this moisture underwent melt mixing and extrusion to fabricate the filaments used for FDM.

A combination method of solution and melt mixing is required when PU cannot be combined with their composites directly using either melt mixing or solution mixing. Solution mixing is typically employed to produce a composite film which is cut into small pieces. Those composite pieces then undergo melt mixing in an extruder to prepare 3D filaments, as shown in Fig. 4.

The combination of solution and melt mixing method is typically employed to prepare feedstock materials based on PU composites for FDM. Evans et al. [61] applied this method to mix TPU and zeolitic imidazolate framework (ZIF- 8) for the production of 3D filaments. TPU filaments were dissolved in dimethylformamide (DMF) while stirred to make a TPU solution. ZIF-8 powders were added in acetone by bath sonication to create a metal- organic framework (MOF) solution. TPU solution was then mixed with MOF solution, and acetone content was reduced from this mixture via rotary evaporation. This mixture was cast onto a dish, and then placed on a hot plate to remove the solvents. The composites were dried in a vacuum oven to prepare composite films that were further cut into small pieces and loaded into the heating barrel of an extruder. In this extruder, composite pieces underwent a melt mixing process, and were extruded into 3D filaments. The solution and melt mixing process were also used by Xiang et al. [67] to prepare a mixture from TPU, CNTs and silver nanoparticles (AgNPs). Nonetheless, TPU was in the powder form instead of filament in this work. The nanocomposite sheets prepared in such a process were chopped into small granules, underwent a melt mixing process using a single-screw extruder, and were extruded into filaments for subsequent FDM printing.

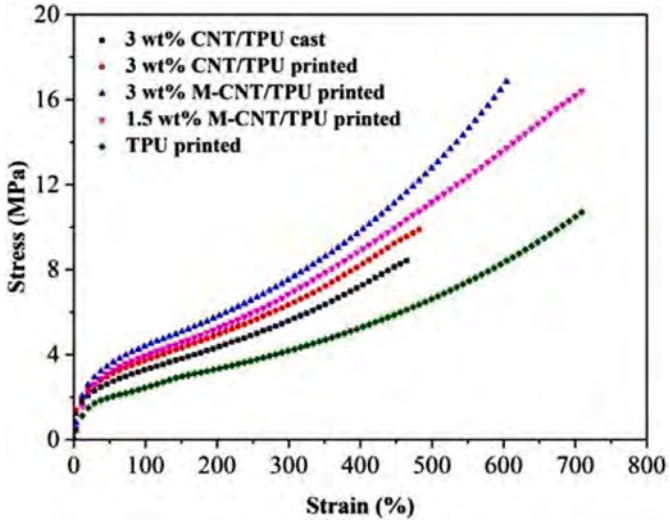

Fig. 5. Stress-strain curves of TPU/MWCNT nanocomposites [62].

Melt mixing is a simple blending method, which is less complicated, expensive and time-consuming than solution mixing despite its low homogeneity level for filler dispersion. Filler dispersion in polymer matrix affects the properties of composites such as mechanical strength, electrical conductivity and thermal conductivity. Therefore, a combination of solution and melt mixing method is necessary to overcome the drawback of the melt mixing process alone. Nevertheless, such a combined method requires more materials (i.e. solvents) and equipment.

3.2. Microstructure and property of 3D printed PU composites

PU with its unique characteristics possesses the specific properties between plastics and rubbers that are widely used in 3D printing to produce some useful parts such as flexible sensors and actuators [81,82]. Even though 3D printed PU may have geometric complexity, the lack of mechanical strength and functionality may still be a major challenge to its widespread applications. To overcome this issue, PU is combined with various materials such as particles, fibres and polymers.

The printed parts result from the combination of PU and other materials to generate unique microstructures, thus impacting the properties of final parts. The relationships between the reinforcement or filler content, microstructure and resulting properties are discussed in detail in this review.

3.2.1. Particle reinforced PU composites

Particle reinforcements are typically used to improve PU matrix properties due to their low cost and easy processability with PU via melt mixing, solution mixing or a combination of melt and solution mixing. The reinforcements using nanoparticles such as CNTs enable to increase tensile strength, Young's modulus, electrical and thermal conductivity [58,62,65,67–69]. Whereas another particle like cork may be employed to reduce density and thermal conductivity [59].

Xiang et al. [62] revealed that the addition of 3 wt% MWCNTs in TPU matrix could enhance tensile strength and Young's modulus of unmodified and modified composite samples up to 39 and 49%, respectively (Fig. 5). This improvement might be related to the disentanglement and alignment effects. The disentanglement diminished particle agglomeration and improved filler distribution in the matrix so that it increased the printed sample elongation. The alignment of each layer resulting from FDM process promotes laminate structures, mainly in the longitudinal direction, which is in the same direction as that of tensile load. Hence, such an alignment can enhance elastic modulus and tensile strength. The surface modification of MWCTs non-covalently by using 1-pyrenecarboxylic acid (PCA) was aimed to improve polymer-nanofiller interactions [83]. Good interaction between polymer matrix and nanofillers can occur when the filler's surface well stick on the matrix material's surfaces to form an excellent unit cell of the composites without any presence of voids, overlaps or other defects. Two particular methods may be proposed to improve the interfacial properties of composites, consisting of covalent and non-covalent modifications. Unfortunately, covalent modification often ruins the intrinsic structures of nanofillers, resulting in the deterioration of mechanical and electrical properties of nanofillers. In contrast, non-covalent modification can improve the interfacial interactions without damaging the structural and physical characteristics of nanofillers [62]. However, another study conducted by Tzounis et al. [58] revealed that when the MWCNT content was increased up to 5 wt%, the tensile strength of composite samples dropped approximately 72.24%, but Young's modulus was raised 20.17%. The decreased tensile strength value may be induced by the weak interfacial strength (adhesion) of the interlayer bonds or the existing CNT microaggregates in such high filler content levels leading to detrimental defects or stress concentration points.

SWCNT nanoparticles have been applied to wrap TPU, known as SWCNT wrapped TPU powders (SWCNT-w-TPU) in order to increase the

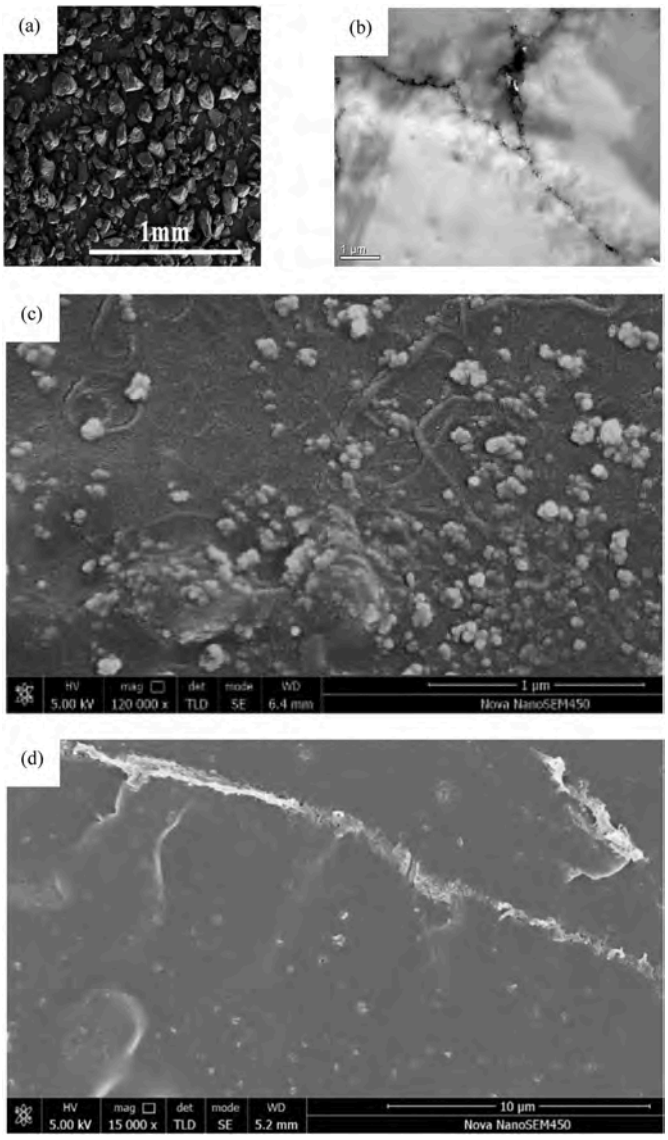

Fig. 6. SEM image identified for (a) 0.2 wt% SWCNT-w-TPU powders, (b) TEM image of 0.2 wt% SWCNT/TPU printed composites, (c) SEM image of 0.2 wt% SWCNT-w-TPU powders surface and (d) SEM image of 0.2 wt% SWCNT/TPU printed composites [69].

electrical conductivity of printed composites via solution mixing process [84]. Such a composite solution was used to fabricate a surface porous macrostructure with the conductive-segregation microstructure used as a flexible piezoresistive sensor via SLS printing [69]. The characterisation of composite powders was performed by capturing SEM and TEM images, as displayed in Fig. 6. Fig. 6a showed that SWCNT-w-TPU powders possessed irregular, but relatively uniform shape, which were similar to TPU powders. Individually dispersed SWCNT particles were adsorbed on TPU powder surfaces, which confirmed that the wrapping structure of SWCNT-w-TPU was a key to the creation of conductive segregation network structure in the matrix (Fig. 6c). Similar to other 3D printing techniques, SLS deposits feedstock materials in a layer-by-layer manner [78]. Therefore, when it processes SWCNT-w-TPU powders, interfacial TPU melt flows across interfacial SWCNT particles, and then coalescences among the adjacent polymer particles. The TPU melt has a high viscosity so that near-zero shear stress of melt flow cannot significantly alter the dispersion morphology of SWCNT particles in the printing process. Hence, these particles remained at the particle boundaries and built conductive segregated networks. Fig. 6b and

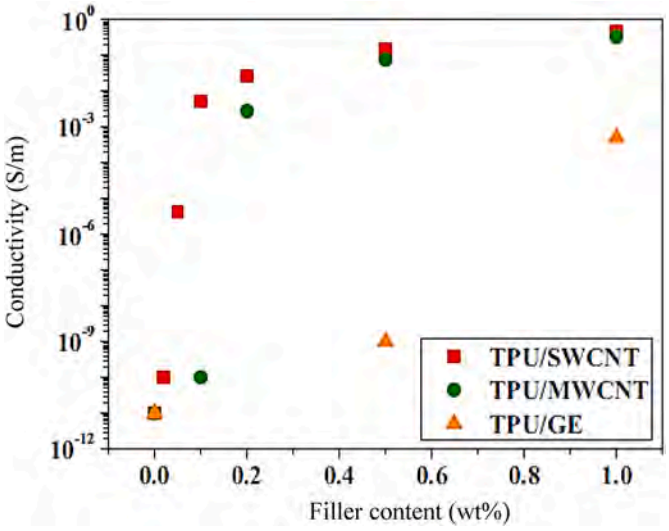

Fig. 7. Electrical conductivity of TPU composites reinforced with different fillers [69].

d displayed the formation of a conductive path of SWCNTs in TPU matrix along with a width of 0.1–0.2 μm to be considered as part of conductive segregation network [69]. Unfortunately, the whole network structure could not be clearly observed solely by using SEM or TEM due to enormous size difference between the network and conductive path.

The effect of SWCNT content on electrical conductivity of printed samples using filler wrapped TPU powders was compared with that arising from other fillers such as MWCNTs and graphene (GE) (Fig. 7) [69]. The additional filler content generated different conductivity effect for those particles. It could be associated with the electrical percolation threshold of the resulting composites. Conductive percolation threshold for TPU/SWCNT composites, TPU/MWCNT composites and TPU/GE composites were 0.05, 0.2 and 1 wt%, respectively. Therefore, the addition of SWCNTs up to 0.05 wt% dramatically increased the electrical conductivity of printed composites. Overall, the electrical conductivity of TPU/SWCNT composites was much higher than that of TPU/GE composites, and slightly higher when compared with that of TPU/MWCNT composites, which was especially true at low filler contents below 1 wt%. Besides, increasing the MWCNT content also improved thermal conductivity of TPU/MWCNT composites [58]. Even though the observed composite samples exhibited relatively low thermal conductivity values (i.e. 0.22–0.55 W $m^{-1}{\cdot}K^{-1}$), the addition of 5 wt% MWCNTs in TPU matrix enabled to enhance the thermal conductivity of the printed composites up to 100% as opposed to 3D printed TPU [58].

The addition of cork in TPU matrix reduces the density and thermal conductivity of neat TPU that suits the specific application like material insulation [59]. Fig. 8 displayed the SEM images of the surface and cross-section of filaments, in which F- 0 and F-5 indicate the cork contents of 0 and 5 wt%, respectively. Increasing cork content enhanced surface roughness of filaments. This trend may be attributed to insufficient impregnation of cork powders by using TPU. Stepashkin et al. [85] suggested that such insufficient impregnation linked to the short residence time of the mixture (i.e., melted polymer and fillers) in the filament extruder. The properties of 3D printed TPU/cork composite are listed in Table 3.

The addition of cork generally decreased the density of composite materials [86], as indicated in Table 3. The density of neat TPU (0 wt% of cork) was 316 kg m^{-3} as opposed to 245 kg m^{-3} for TPU composites reinforced with 5 wt% cork with a typical decline of 22.47%. A similar result was obtained by Daver et al. [87] for printed PLA/cork composites and by Brites et al. [88] for printed high-density polyethylene (HDPE)/cork composites. The decreasing density in printed composites could be caused by the presence of voids between the cork and TPU

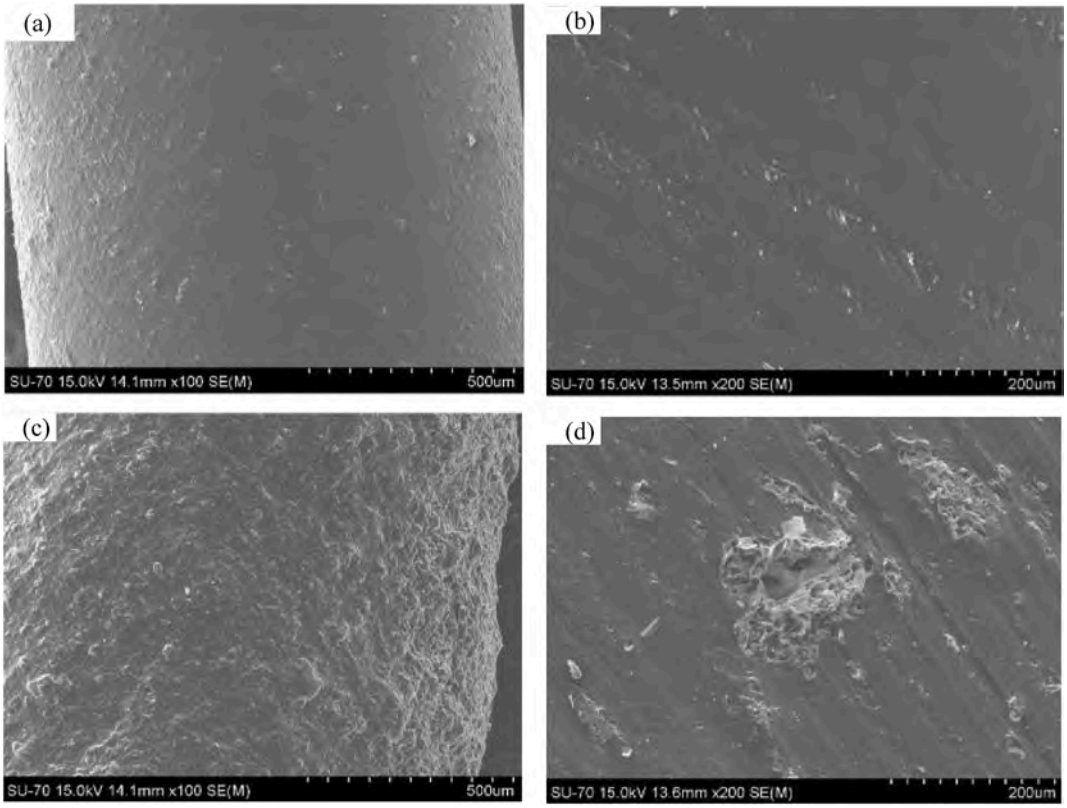

Fig. 8. SEM images of the filaments: (a) surface of F-0 cork, (b) cross-section of F-0 cork, (c) surface of F-5 cork, (d) cross-section of F-5 cork [59].

Table 3
Properties of 3D printed TPU/cork composites [59].

Property	3D printed structure-0 cork	3D printed structure −1 cork	3D printed structure −3 cork	3D printed structure −5 cork
Density ($kg{\cdot}m^{-3}$)	316 ± 4	262 ± 4	252 ± 3	245 ± 3
Thermal conductivity ($W.m^{-1}{\cdot}K^{-1}$)	0.049 ± 0.000	0.047 ± 0.000	0.047 ± 0.000	0.044 ± 0.001
Specific heat ($J{\cdot}kg^{-1}{\cdot}K^{-1}$)	305 ± 7	325 ± 8	320 ± 4	262 ± 11
Thermal diffusivity ($m^2{\cdot}s^{-1}$)	5E-7 ± 8E-9	6E-7 ± 1E-8	6E-7 ± 5E-8	7E-7 ± 4E-8
Thermal effusivity ($Ws^{1/2}\ m^{-2}\ s^{-1}$)	69 ± 1	64 ± 1	61 ± 1	52 ± 3
Young's modulus (kPa)	2278 ± 83	782 ± 19	711 ± 11	703 ± 19
Compressive stress at 10% (kPa)	169 ± 6	71 ± 1	55 ± 3	22 ± 3
Toughness ($J{\cdot}m^{-3}$)	508 ± 23	316 ± 5	309 ± 6	251 ± 5

matrix in the composite unit cell with respect to the 3D filament. When this filament is extruded and deposited layer by layer onto the build platform, other voids may be formed among adjacent layers in the similar ply and between layers at different ply (above and below). Consequently, the increasing void number lowers the mechanical properties of composite structures such as Young's modulus, compressive strength and toughness.

Table 4 summarises various particles used to reinforce PU composites in 3D printing, as well as improved properties of resulting composites. CNTs, mainly MWCNTs, can be considered as effective

Table 4
Summary of enhanced properties in 3D printing of PU composites reinforced by different particles.

Method	Material system	Optimum filler content	Improvement in properties	Ref.
FDM	TPU/cork	5 wt% cork	Reducing density and thermal conductivity of the printed components	[59]
	TPU/ MWCNT	3 wt% MWCNTs	Enhancing tensile strength, strain, and gauge factor (GF)	[62]
		5 wt% MWCNTs	Improving tensile, Young's modulus, and electrical conductivity	[65]
		5 wt% MWCNTs	Increasing thermal conductivity	[58]
	TPU/ MWCNT/ AgNP	3 wt% MWCNT/ AgNP	Improving elastic modulus	[67]
SLS	TPU/CNT	1 wt% CNTs	Enhancing electrical conductivity	[68]
SLS	TPU/ SWCNT	0.05 wt% SWCNTs	Improving electrical conductivity	[69]

reinforcements in TPU matrix as opposed to other particles due to their unique characteristics to improve the properties of pristine TPU such as tensile strength, elastic modulus, electrical and thermal conductivities [58,62,65,67]. On the other hand, FDM is employed to process TPU composites more frequently than other 3D printing methods. It may lie in the simplicity of this technique and also its ability to process various material successfully in order to facilitate the mixing of different materials such as TPU and its reinforcements.

3.2.2. *Fibre and polymer reinforced PU composites*

Several fibres such as polyolefin fibres and cellulose nanofibres (CNFs), as well as certain polymers like polylactic acid (PLA),

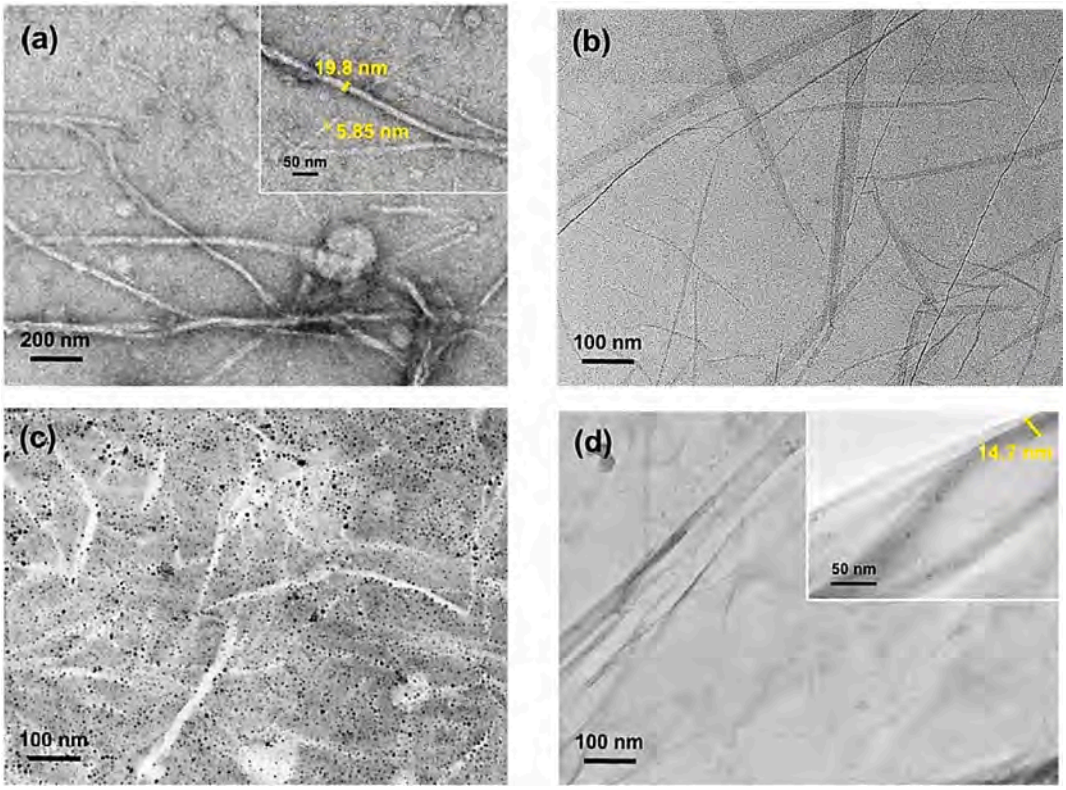

Fig. 9. Different micrographs identified for (a) unmodified CNF, (b) rGO, (c) surface-grafted PEG/CNF composites and (d) surface-grafted CNF/rGO [25].

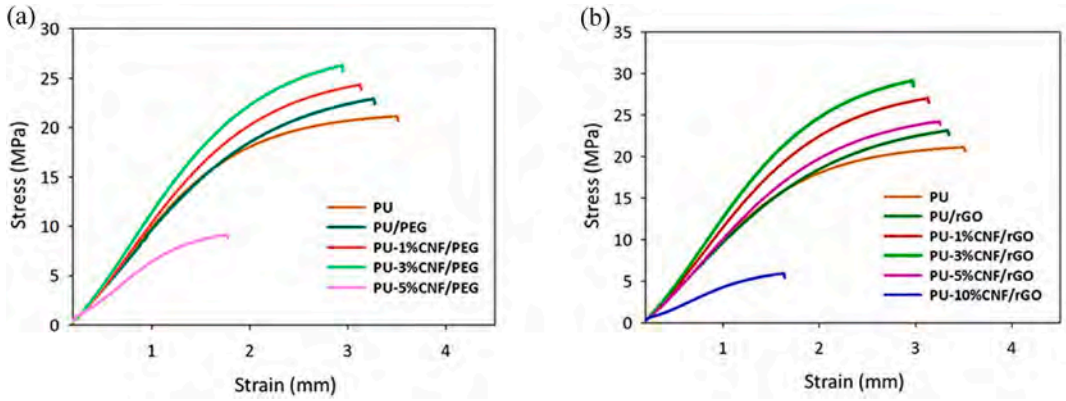

Fig. 10. Stress-strain curve of UV-cured PU and modified cellulose reinforced with (a) PEG and (b) rGO [25].

polyaniline (PANI) and TEGMA have been considered as PU reinforcements to improve mechanical properties (i.e., tensile strength and flexural strength, elasticity modulus and toughness) of composite structures [18,25,66,71,79,89,90]. Other fillers, namely PLA along with graphene oxide (GO), hexagonal boron nitride (hBN) and graphene sheet (GS) are used to increase thermal stability, thermal conductivity and electrical conductivity of printed composites [19,64,70].

Mohan et al. [25] used natural fibres, known as cellulose nanofibrils (CNFs) originating from oil palm empty fruit bunch (EFB) as the fillers in PU matrix to enhance tensile strength of printed composites. CNFs come from sustainable materials (i.e., agricultural waste of palm oil mill). This waste containing rich lignocellulose that can be processed becomes nanocellulose, especially for reinforcing fillers in polymer matrix [91]. Nevertheless, CNFs should be treated to improve their compatibility with UV-curable PU-based resin since such fibres were used as the feedstock materials for DLP printing. Therefore, the surface hydrophilicity of CNFs is adapted with polyethylene glycol (PEG) and reduced graphene oxide (rGO) to prepare a good mixture in combination with UV-curable PU resin.

The micrographs for the cross-section of printed samples, observed by a field emission scanning microscope (FE-SEM), were shown in Fig. 9. Fig. 9a indicated the successful cellulose defibrillation where individual fibrils possessed a comparable average-diameter range from 5 to 20 μm [92]. Conversely, rGO appeared to be a semi-transparent sheet material, which became unstable under the TEM observation (Fig. 9b). Disordered and unwrinkled structures could be ascribed to the non-removal of oxygen atoms, as well as a high degree of exfoliation during the oxidation [93]. Fig. 9c presented the micrograph of PEG/CNF composites with respect to the dispersibility of CNFs within PEG matrix. On the other hand, Fig. 9d displayed the visible trace of CNFs under a thin layer of rGO [94]. The modified CNFs were found to exhibit the stability of interfacial agents while remaining as individual fibrils.

The dispersibility of modified CNFs in UV-cured PU was studied using tensile properties of materials, as shown in Fig. 10. The addition of

Fig. 11. Synthetic fibre surface after bond strength tests: (a) plain fibre (uncoated), (b) PU resin-coated fibre and (c) UF resin-coated fibre [79].

PEG and rGO to PU containing 1 wt% modified CNFs increased the tensile strength by 8.3% and 9.37%, respectively [25]. It might be explained by the fact that PEG/CNF and CNF/rGO could facilitate the crystallisation process of PU in their composite systems [95]. Graphene is a popular carbon-based nanofiller since its layered structures yield very large surface areas (up to 2630 $m^2\ g^{-1}$) [96]. Therefore, a lower loading of such fillers may promote the properties of composites owing to high aspect ratios of fillers [97]. As evidently shown in Fig. 10, it was revealed that PU-3%-CNF/PEG composites had higher tensile strength by approximately 24% when compared to that of neat PU. PU-3%-CNF/rGO composites even possessed an increase in tensile strength by 37% and 11% when benchmarked against those of PU and PU-3%-CNF/PEG composites. Even though the addition of PEG facilitated the interaction between hydrophilic CNFs and hydrophobic PU, rGO could provide better removal of CNF hydrophilicity, as opposed to PEG because of a higher density of carbon atoms on its surface [98,99]. rGO may lose natural hydrophilicity of CNFs so that it allowed CNFs to disperse well within hydrophobic PU matrix [100]. Meanwhile, the loading of 5 wt%% modified CNFs decreased the tensile properties due to resulting non-uniform stress transfer when composite samples were subjected to tension loading. It appeared that when the filler loading reached 5 wt% or above, CNFs tended to aggregate in PU matrix and generate more interfacial voids to deteriorate the tensile strength of composites [101]. Besides, a higher CNF loading might interrupt the curing process of photocurable PU resin, and further affected the orientation of printed samples due to insufficient curing.

In addition to CNFs, polylactic acid (PLA) can be used as the reinforcements to improve the tensile strength and elastic modulus of PU [89]. Besides, PLA combined with GO enables to enhance thermal stability [19] and when this polymer is mixed with triethylene glycol dimethacrylate (TEGDMA) and graphene, such reinforcements enable to increase the flexural strength of PU accordingly [18]. Chen et al. [19] employed PLA and GO to reinforce PU matrix and manufactured biocompatible TPU/PLA/GO nanocomposites by using FDM. This work was intended to produce the printed composite structures with excellent biocompatibility to NIH3T3 cells. The printed composites showed a great potential as biomaterial scaffolds for tissue engineering applications.

Interfacial toughness of printed composites could be enhanced by using synthetic polyolefin fibres as the core and PU resin, as well as urea-formaldehyde (UF) resin as the core coating material [79]. It intended to enhance the hydrophobicity of synthetic fibre surfaces and improve the interfacial toughness of composite structures. Solution mixing method as well as DIW and DLP printing were applied to blend the fillers with the matrix in order to manufacture resulting composite samples.

Fig. 11 displays surface images of extracted fibres for three conditions, namely uncoated fibres, PU resin-coated fibres and UF resin-coated fibres. In particular, pull-out uncoated fibres encountered scratches and severe damages (Fig. 11a). Conversely, for coated fibres using PU and UF resin, the fibre surface exhibited less damage (Fig. 11b and c). It confirmed that the shell material reduced the degree of damage to the core material. When compared to PU, UF could provide a better coating to synthetic fibre surfaces, in which it was supported by relevant results of bond strength tests, as illustrated in Fig. 12. This figure revealed that fibre-reinforced PU composites possessed lower bond strength and interfacial toughness relative to plain mixture (Fig. 12a). It could be caused by the poor adhesion between polyolefin fibre surfaces and PU matrix owing to the existence of voids in composites. Consequently, it reduced both bond strength and interfacial toughness of such composites. In contrast, UF fibre treatment was suggested to increase bond strength by 134% and interfacial toughness by 147%, as opposed to those of plain mixture (Fig. 12b) [79]. It was implied that the combination of UF and synthetic fibres could yield strong interfacial adhesion.

Polyaniline (PANI) can be employed to improve the electrical conductivity of printed composites fabricated by DLP that may be applied in biomedical fields such as sensors and antistatic materials in biomedical devices [70]. Fig. 13 presents FE-SEM images of printed composites with different PANI content. Increasing the PANI content yielded a larger area of PANI embedded in TPU matrix leading to intermaterial aggregation.

The aggregation of PANI was associated with strong hydrogen

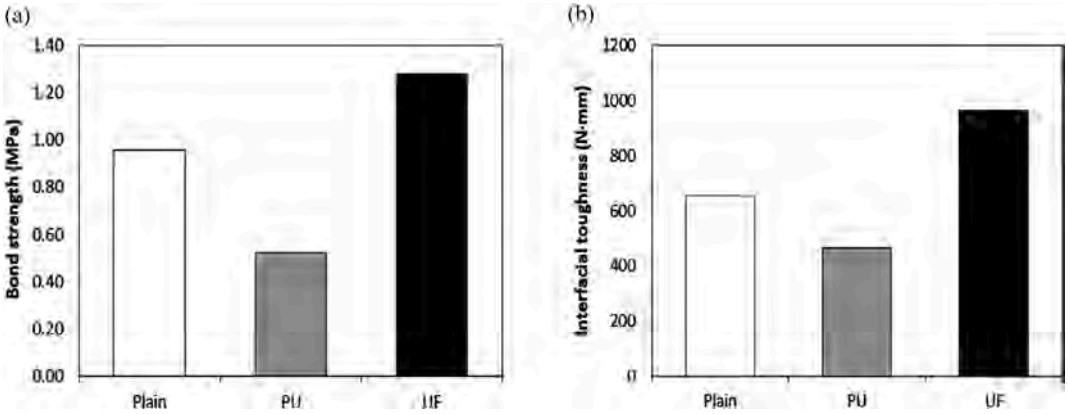

Fig. 12. Self-healing bonding behaviour of cementitious composites: (a) bond strength, (b) interfacial toughness [79].

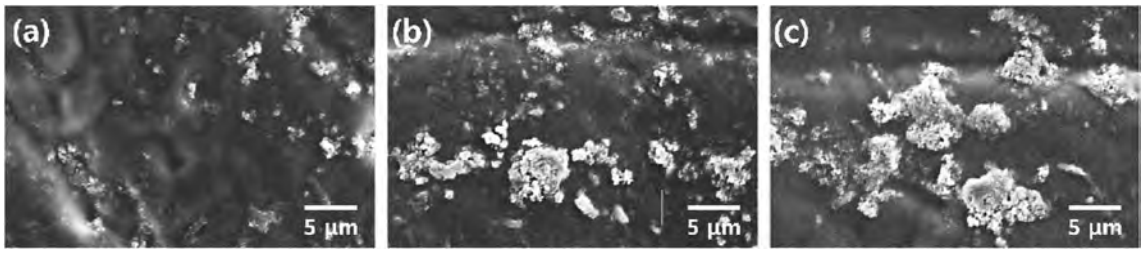

Fig. 13. FE-SEM images of printed composite samples at different PANI contents: (a) 1 wt%, (b) 3 wt% and (c) 6 wt% (Courtesy of the U.S. National Library of Medicine) [70].

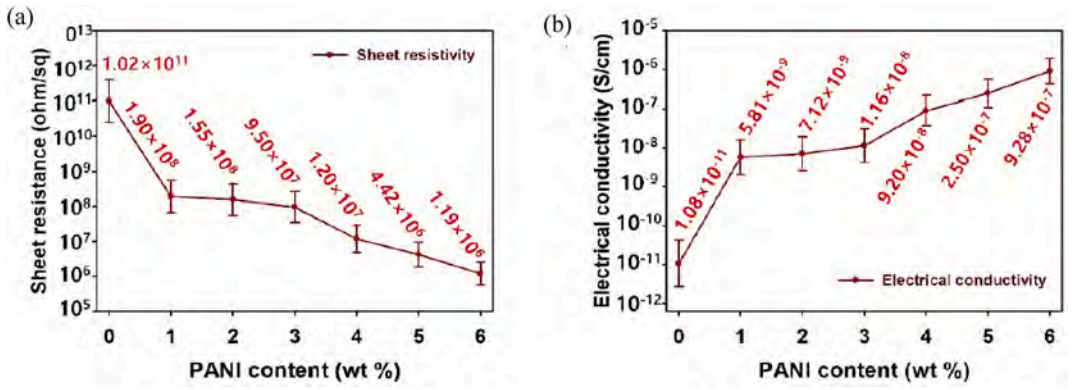

Fig. 14. (a) Resistance and (b) electrical conductivity of printed composite samples (Courtesy of the U.S. National Library of Medicine) [70].

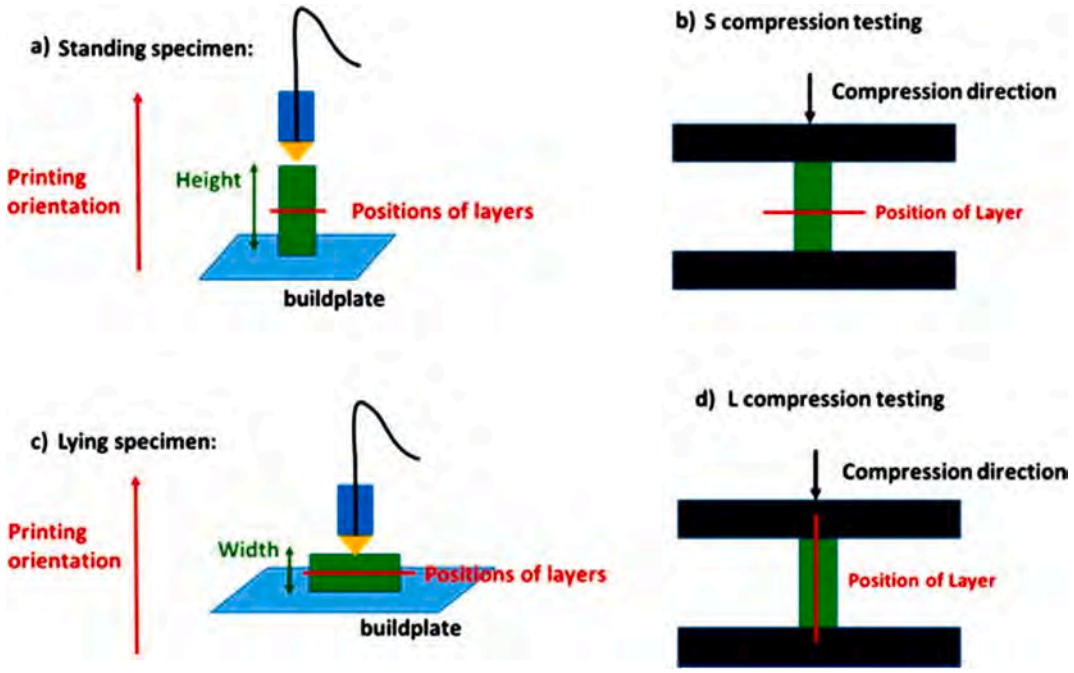

Fig. 15. Schemes of different orientations with respect to printing and compression tests of specimens: (a) standing specimens, (b) *S* compressing testing, (c) lying specimen and (d) *L* compression testing. Reprinted with permission from Ref. [19]. Copyright 2017 American Chemical Society.

bonding, London force [70] between PANI chains and dipole-dipole [102,103]. The aggregation of PANI disturbed the crosslinking process between PU prepolymers [104] so that the maximum content of PANI in printed composites was fixed at 6 wt%. The sensitivity of composite samples declined with increasing the PANI content. The lowest composite resistance and the highest electrical conductivity of printed samples were achieved when the PANI content was 6 wt% (Fig. 14). Under this condition, the resistance and electrical conductivity of PANI/TPU composites reached 8.57×10^4 times lower (i.e., 1.19×10^6 $\Omega \cdot sq^{-1}$) and 8.57×10^4 times higher (9.28×10^{-7} S cm^{-1}) than those of pure TPU accordingly. It indicated that the incorporation of PANI nanoparticles enabled to create conductive channels for electron delocalisation in TPU matrix [105–107].

The effect of printing orientation on microstructures and tensile

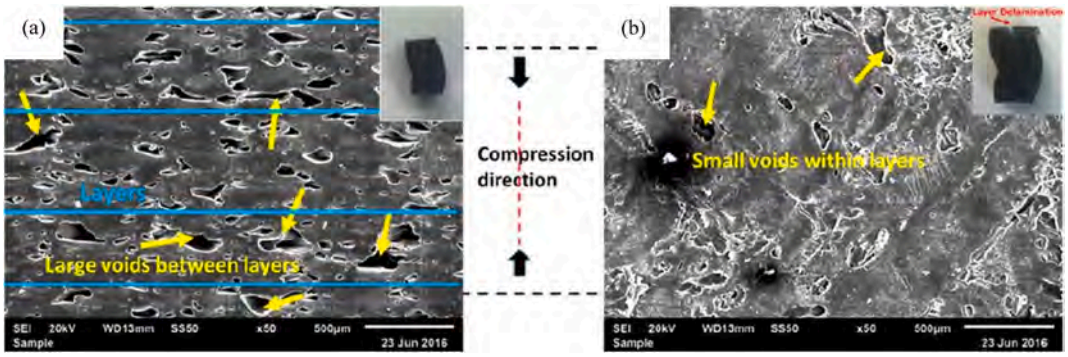

Fig. 16. SEM images of diverse cross-sections of different composite samples reinforced with 0.5 wt% GOs: (a) *S* sample and (b) *L* sample. Adapted with permission from Ref. [19]. Copyright 2017 American Chemical Society.

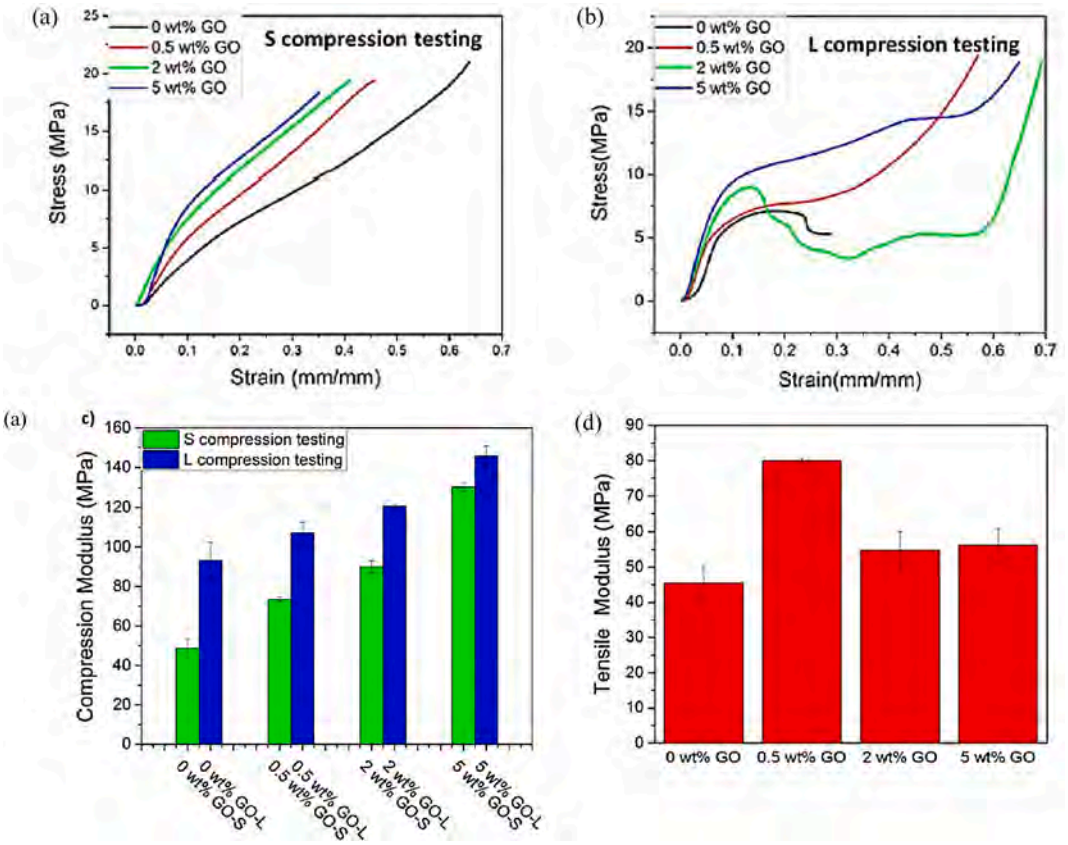

Fig. 17. (a) Compression testing curve of *L* sample, (b) compression testing curve of *S* sample, (c) compression moduli of *S* and *L* samples and (d) tensile modulus at different GO loadings. Adapted with permission from Ref. [19]. Copyright 2017 American Chemical Society.

modulus, as well as yield strength of printed structures have been investigated by Chen et al. [19]. The orientations of the specimen subjected to printing and compression tests were shown in Fig. 15. The printing orientations with the standing specimen (*S*) and lying specimen (*L*) were illustrated in Fig. 15a and c, respectively. The printing orientation for standing specimen was the same as the height direction while for lying specimen it was the same as the width direction. The compression testing was applied to both types of specimens in a way where the height direction was parallel to the compression orientation (Fig. 15b and d).

The cross-section of the *S* sample contained multi-layers that were packing together. It was observed that a significant number of voids appeared between different layers (Fig. 16a). In contrast, for the cross-section of the *L* sample, only a limited number of voids were identified in one individual layer (Fig. 16b).

Fig. 17a, b and c revealed that the modulus of *S* compression for each sample was smaller than that of *L* compression. In *L* compression, the stress underwent a decrease especially in the GO loading range of 0–2 wt %, while the samples tended to fail at the final stage. Conversely, the stress continued to increase in *S* compression until the samples failed. FDM built the printed samples by depositing materials onto the build platform in a layer-by-layer manner. The adhesion between two adjacent layers was associated with physical interaction, allowing air to be trapped in contact areas among layers so that it caused the voids and loosened the packing of layers [19]. The loose packing and the presence of large voids between layers in the *S* compression tests yielded smaller compression modulus when compared to those in the *L* compression tests. It confirmed the presence of the effect of the printing orientation on mechanical properties, which is also known as anisotropic effect in FDM. The incorporation of GO particles in PLA/TPU matrix increased

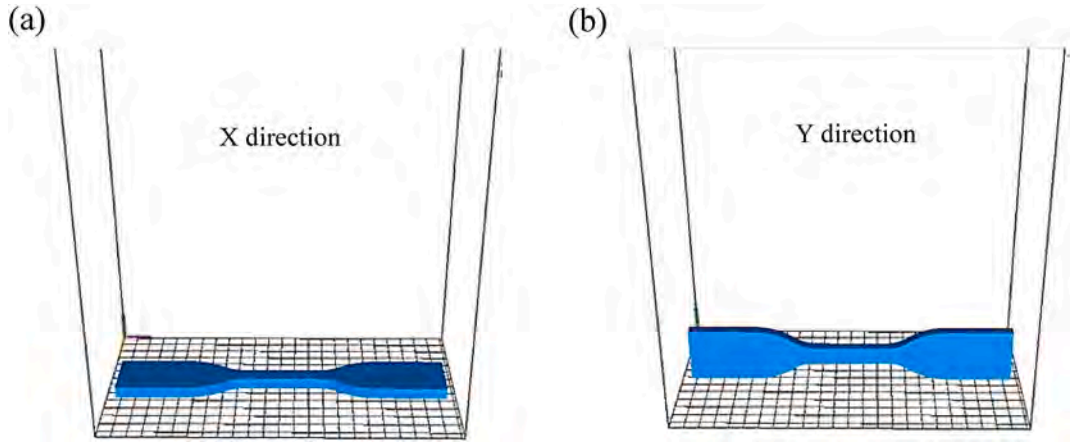

Fig. 18. Printing orientation of PU/PLA/TEGDMA composite sample: (a) X direction (face up) and (b) Y direction (edge up) [18].

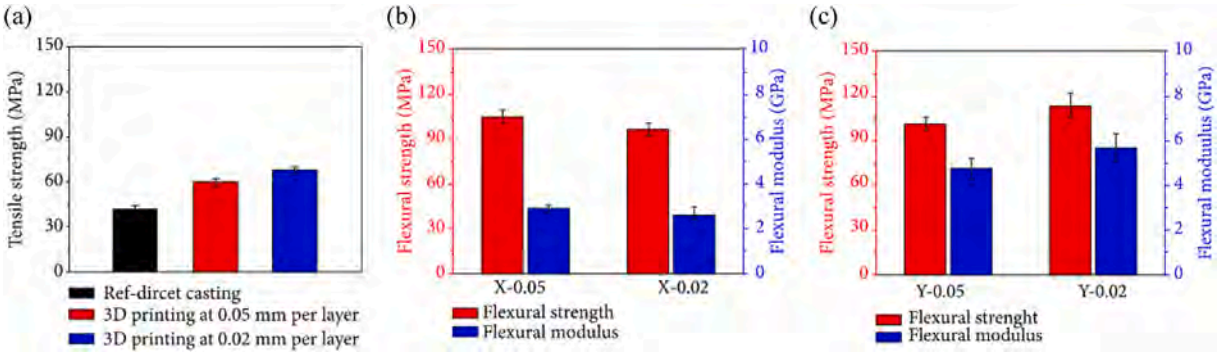

Fig. 19. Effect of layer thickness and printing orientation on: (a) tensile strength, (b) flexural strength and (c) flexural modulus of composite samples fabricated by SLA compared to those produced by direct casting [18].

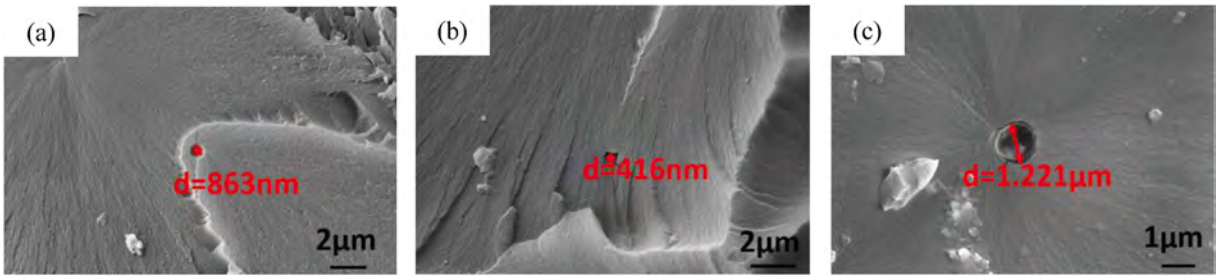

Fig. 20. SEM images of tensile fractured surfaces, a bubble in (a) X-0.02 sample, (b) X-0.05 sample and (c) direct casting sample [18].

tensile modulus of nanocomposite samples. In particular, at the GO loading of 0.5 wt%, tensile modulus could be enhanced by 75.50% relative to that of pristine PLA/TPU composites (Fig. 17d). However, beyond 0.5 wt% GO, both tensile modulus and yield strength decreased, possibly resulting from a decrease in the elasticity of polymer matrix.

The effect of layer thickness and printing orientation of printed composites derived from PLA-PU oligomer and TEGDMA and manufactured by SLA, on the tensile and flexural strength and flexural modulus, was studied by Feng et al. [18]. Printing orientation of the composite samples is shown in Fig. 18.

The printing accuracy affects the mechanical properties (i.e. tensile and flexural strength as well as flexural modulus) of the printed composites, as indicated in Fig. 19. Samples manufactured by a conventional method of direct casting exhibited relatively poor mechanical properties due to larger visible bubbles when compared with those produced by SLA (Fig. 20). The bubble size resulted from direct casting was approximately 1.4 and 2.9 times bigger than that generated by SLA (X-0.02 and X-0.05).

The tensile strengths of composite samples printed in X-direction with a layer height of 5 mm and 2 mm (X-00.5 and X-0.02) were 43 and 62% higher than that fabricated by direct casting (Fig. 19a). It could be related to the presence of bubbles to break the bonds between particles of PU, PLA and TEGDMA so that it further lowered the tensile strength of laminate structures [18]. Printed composite samples with a layer thickness of 2 mm (X-0.02) generated bigger bubbles than that of 5 mm (X-0.05) (Fig. 20). Consequently, it reduced the flexural strength and flexural modulus of printed composites, as displayed in Fig. 19b. Conversely, in the Y-direction, printed composite samples with a layer thickness of 2 mm (Y-0.02) had higher flexural strength and flexural modulus than Y-0.05 due to typical shrinkage effect. This effect created more defects on Y-0.05 samples as opposed to Y-0.02 resulting in the decrease in mechanical strength of composite structures.

Table 5
Summary of property enhancement in 3D printed PU composites reinforced with fibres and polymers.

Method	Material system	Optimum filler content	Improvement in properties	Ref.
FDM	TPU/PLA	20 wt% PLA	Increasing the tensile strength	[66]
		70 vol% PLA	Improving the tensile strength and elasticity modulus	[89]
		75 wt% PLA	Enhancing tensile strength	[90]
	TPU/PLA/GO	0.5 wt% GO	Increasing tensile modulus and thermal stability	[19]
	TPU/hBN	40 wt% hBN	Enhancing thermal conductivity	[64]
DIW	• Polyolefin fibre/ urea-formaldehyde resin (UF) • Polyolefin fibre/ PU resin	5 wt% sodium silicate	Improving the interfacial toughness	[79]
DLP	PU/CNF/reduced graphene oxide (rGO)	3 wt% cellulose nanofibres (CNFs)	Enhancing the compatibility of mixture solution with the UV-curable PU resin and the tensile strength at the CNF content below 3 wt %	[25]
	PU/CNF/graphene nanoplatelet (GNP)	0.6 wt% lignin/ graphene	increasing tensile strength and hardness	[71]
	• PU/polyaniline (PANI) • PU/graphene sheet (GS)	• 6 wt% PANI • 2 wt% GS	Improving the electrical conductivity	[70]
	PLA-PUA/ TEGDMA/ graphene	• 37 wt% TEGDMA, 62 wt% PLA-PUA, 1 wt% Irgacure 819, and 0.5 wt % graphene • 3D printing with the layer thickness of 0.02 mm and X-axis direction	Enhancing the tensile and flexural strength	[18]

The summary of improved properties of PU composites reinforced with fibres and polymeric materials are listed in Table 5. Three different techniques (i.e. FDM, DIW and DLP) have been used to process PU composites reinforced with fibres and polymers. Both types of reinforcements could improve mechanical, electrical and thermal properties of printed samples. PLA, graphene and TEGDMA are commonly utilised to enhance tensile and flexural strengths, elastic modulus, as well as thermal stability [18,19,66]. Whereas hBN, polyolefin fibres, CNFs and PANI enable to enhance thermal conductivity, interfacial toughness, compatibility with UV-curable resin and electrical conductivity, respectively [25,64,70,79]. Increasing the filler content does not always improve the properties of composite samples. When the addition of fillers or reinforcements exceeds certain optimum values as the threshold level (Table 5), it may diminish the properties of printed parts.

As mentioned in Table 5, the addition of 20 and 75 wt% PLA [66,90] in the TPU matrix can improve the tensile strength. The different experimental conditions between both studies mainly take place in the step of filament fabrication. Leng et al. [66] used the mass ratio of TPU and PLA as many as 80:20 and extruded the TPU/PLA mixture twice to yield good composite filaments using a twin screw extruder and a single screw extruder. Whereas Tao et al. [90] extruded the TPU/PLA mixture four times to obtain a well-mixed composite filaments with the aid of single screw extruder. The printed sample with 75 wt% PLA yielded higher tensile strength compared to composite counterpart containing 50 wt% PLA.

3.2.3. Modifier effect in the printed PU composites

The modifier is typically used to improve the interfacial adhesion between the fillers and the matrix, as revealed by previous studies [108–111]. For instance, five different modifiers, namely maleic anhydride grafted ethylene- propylene- diene- monomer (EPDM-g-MAH), maleic anhydride-grafted polyolefin elastomer (POE-g-MAH), polyethylene glycol (PEG) 6000, chitosan and diphenylmethyl propane diisocyanate (MDI), were added to improve the interfacial adhesion between wood flour (WF) as the fillers and TPU matrix. The addition of those fillers succeeded in improving the tensile strength of printed composites [63]. WF is a kind of biomass material and available almost everywhere. Therefore, WF is a good filler candidate as low-cost natural fibres, as well as biodegradable and eco-friendly materials. The fracture surface morphologies of composite samples at different WF contents in range from 0, 10, 20, 30 to 40 wt% and with or without modifiers are shown in Fig. 21.

The fracture surface gaps between WF and TPU in composites modified by POE-g-MAH, PEG 6000 and chitosan (Fig. 21c–e) increased compared to unmodified counterparts (Fig. 21a). These results were also detected by Adsuar et al. [112] and Alves et al. [108]. In contrast, with the addition of EPDM-g-MAH (Fig. 21b) and MDI (Fig. 21f) modifiers, WF was apparently wrapped up by TPU matrix with a clear sign of consistent interfaces. The fracture gaps between them were narrower than those of unmodified TPU/WF composites. It indicated that EPDM-g-MAH had improved interfacial adhesion on resulting composite structures.

The MDI modified composites exhibited the highest tensile strength, which increased by approximately 22.33% compared to unmodified TPU/WF composites (Fig. 22). It could be induced by a strong intermolecular interaction between MDI and the matrix. The isocyanate groups in the MDI structure reacted with hydroxyl groups in WF and carbamate groups in TPU molecular structures to yield carbamates. It increased the bonding force between TPU and WF leading to the enhanced tensile strength. EPDM-g-MAH modified composites showed the largest elongation at break along with excellent compatibility [108,113]. Such a finding could be associated with close interaction between WF and EPDM-g-MAH in composites based on the reaction between -OH groups and maleic anhydride since EPDM may also function as a cross-linker in main chains of TPU [108,114].

3.3. Predicted models

Models for simulation purposes are required to predict composite properties using empirical data in order to reduce the number of trials and eliminate trials that are difficult to be conducted. The simulation processes are developed based on various numerical techniques and algorithms. For instance, Shi et al. [89] employed a rule of mixtures (RoM) to determine the performance of each component and the volume fraction of two components, as indicated in equations (1) and (2), respectively.

$$E_c = E_1 \upsilon_1 + E_2 \upsilon_2 \quad (1)$$

$$\upsilon_1 + \upsilon_2 = 1 \quad (2)$$

E_c, E_1 and E_2 represent the theoretical value of composite material properties and property values (e.g. tensile strength, elongation at break and elasticity modulus) of material constituents 1 and 2. Whereas υ_1 and υ_2 represent the volume fractions of constituents 1 and 2, respectively.

Another model mentioned by Xiang et al. [62] was established to investigate the sensing mechanism based on Simmons' tunnelling theory [115]. The strain sensing response of printed composites greatly

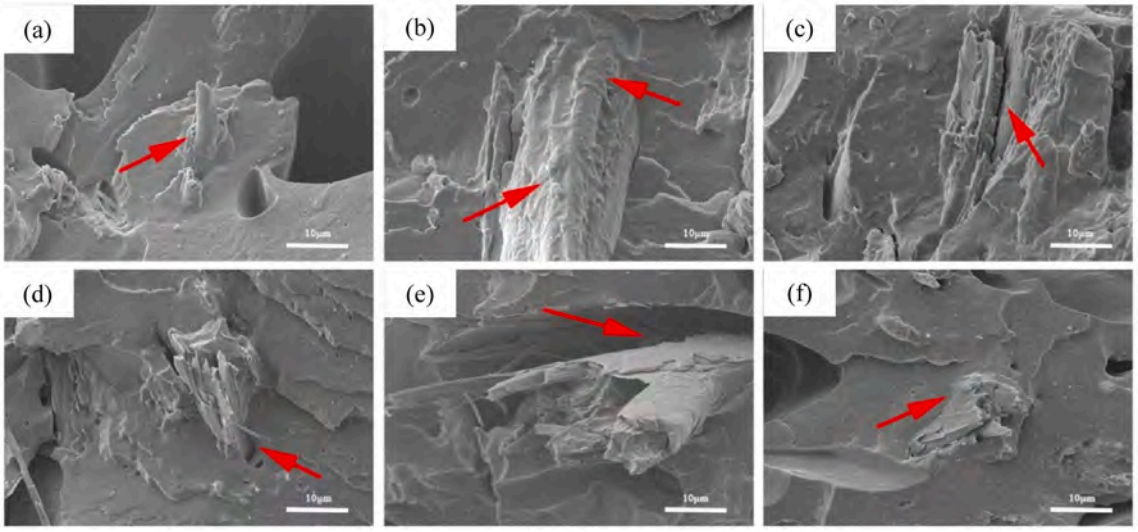

Fig. 21. SEM images of cryofractured TPU/WF composites with the WF content of 20 wt%: (a) Unmodified TPU/WF composites, (b) EPDM-g-MAH modified TPU/WF composites, (c) POE-g-MAH modified TPU/WF composites, (d) PEG 6000 modified TPU/WF composites, (e) chitosan modified TPU/WF composites, (f) MDI modified TPU/WF composites [63].

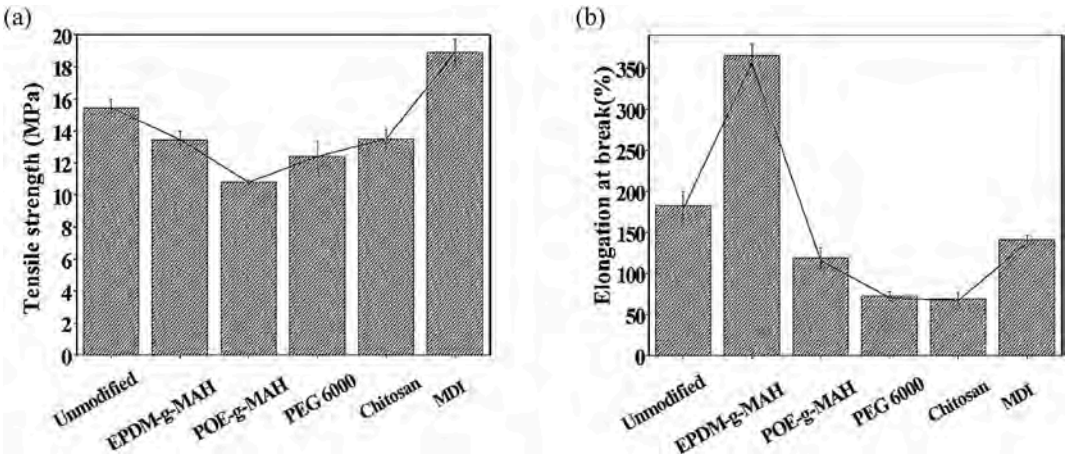

Fig. 22. Effect of different modifiers on (a) tensile strength and (b) elongation at break [63].

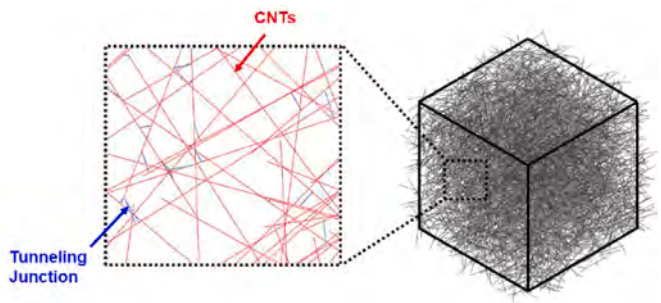

Fig. 23. 3D resistance network model [65].

depends on the destruction and reformation of conductive network [62]. The total resistance (R) of conductive composites can be expressed by equations (3) and (4) together. Such equations have also been used by Xiang et al. [67] to calculate the total resistance of printed PU/CNT/AgNP composites.

$$R = \left(\frac{L}{N}\right)\left(\frac{8\pi hs}{3\gamma a^2 e^2}\right)\exp(\gamma s) \tag{3}$$

$$\gamma = \frac{4\pi\sqrt{2m\varnothing}}{h} \tag{4}$$

L, N and h are the number of particles forming a single conductive path, the number of conductive paths and Planck's constant. Whereas s, a^2, e, m and $\varnothing$ represent the shortest distance between conductive particles, effective cross-section area, electron charge, electron mass and the height of potential barrier between particles [116]. When the printed composites is stretched, the distance between nanofillers linearly increases from s_0 to s, in which it enhances the electrical resistance of printed composites. The shortest distance between nanofillers is calculated according to equation (5).

$$s = s_0\left(1 + C\left(\frac{\Delta l}{l_0}\right)\right) = s_0(1 + C\varepsilon) \tag{5}$$

where ε, l_0, Δl and C are indicative of sensor strain, sensor original length, sensor deformation and a constant that can vary in material systems.

Kim et al. [65] developed a 3D resistance network model to simulate the conduction phenomenon of PU/MWCNT composites using Fortran program and the commercial finite element program (ABAQUS/-standard). The dispersion of MWCNTs was approached with a cubic unit

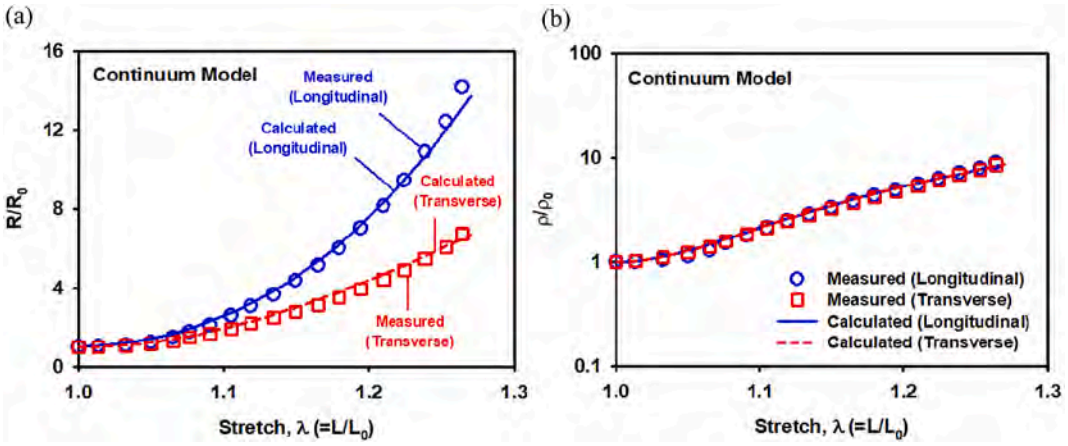

Fig. 24. (a) Normalised resistance and (b) normalised resistivity predicted by continuum resistivity model [65].

cell with a size of 1000 × 1000 × 1000 nm^3, as shown in Fig. 23.

The resistivity evolution of PU/MWCNT composites in this study [65] was modelled in the continuum sense, in which the Ohm's law is given by equation (6), and $\boldsymbol{E}$ as well as $\boldsymbol{j}$ represent the field strength and current density accordingly. The resistivity tensor ($\boldsymbol{\rho}$) is expressed by equation (7), and ρ is a resistivity parameter depending on deformation.

$$\boldsymbol{E}=\rho\boldsymbol{j} \tag{6}$$

$$\boldsymbol{\rho}=\rho\begin{bmatrix}1&0&0\\0&1&0\\0&0&1\end{bmatrix} \tag{7}$$

Fig 24 revealed that the calculated values of normalised resistance (R/R_0) and normalised resistivity (ρ/ρ_0) predicted by the continuum resistivity model based on the stretched function had good consistency with the experimental data both in longitudinal and transverse directions. It means that such a model could become a useful tool to predict piezoresistive behaviour of 3D printed polymer composites.

Buckling phenomenon of filaments in FDM enables to be predicted by using Euler buckling equation [26] as follows:

$$P_{cr}=\frac{\pi^2 E D_f^2}{16 L_f^2} \tag{8}$$

P_{cr}, E, D_f and L_f are critical buckling pressure, filament elastic modulus, filament diameter and filament length from the drive gear to the melting zone. When the filaments are not sufficiently stiff, they can buckle in the region between the drive gear and melting zone and stops

Table 6
Summary of SMPU materials and their composites for 4D printing.

SMPU			Composites			3D printing technique	Ref.
Type	Specification	Supplier	Type	Specification	Supplier		
TPU	• MM3520 • Pellet • Glass transition temperature (T_g): 35°C • Specific gravity: 1.25	SMP Technologies Inc., Japan	MWCNTs	• Length: 100–200 μm • Average diameter: 8 nm	Jeio Co., Incheon, Korea	FDM	[125]
TPU	• DiAPLEX MM 4520 • Pellet • T_g : 45°C • Specific gravity: 1.25	SMP Technologies Inc., Japan	Carbon black (CB)	Ketjenblack, EC600JD	Akzo Nobel, USA	FDM	[126]
TPU	• MM3520 • Pellet • T_g: 35°C • Specific gravity: 1.25	SMP Technologies Inc., Japan	Tungsten	• Powder • Purity: > 99.9% • Size: 0.6–1 μm	Sigma Aldrich	FDM	[129]
Waterborne PU	Rust-Oleum triple thick polyurethane clear matte	Rust-Oleum	• Carbomethyl cellulose (CMC) • Silicon dioxide (SiO_2)	• Whatman CMC pre- swollen microgranular cation exchanger CM52 • Size: 10–20 nm • Density: 2.2–2.6 g mL^{-1} at 25°C	• Whatman-Cytiva • Sigma Aldrich	FDM	[80]
TPU	• Elastollan TPU, 1185A • Tg: −38°C • Specific gravity: 1.12 • Melt flow index: 10–20 g/10 min (190°C, 8.7 kg)	BASF	Polylactic acid (PLA)	• PLA 8052D • Tg:60°C • Specific gravity: 1.24 • Melt flow index: 14 g/10 min (210°C, 2.16 kg)	Natureworks LLC	FDM	[20]
TPU	• Elastomer TPU	Changsha Yitailong, China	PLA	• Shape memory material (SMP)-PLA • Filament diameter: 1.75 mm	Zhejiang Hailuohao, China	FDM	[82]
TPU	• Filament • (T_g): 55°C • Filament diameter: 1.75 mm • Melting temperature: 205-215°C	SMP Technologies Inc., Japan	Nylon	• Plain woven fabric • Thickness: 0.1 mm		FDM	[130]

the printing process. It is noteworthy that P_{cr} of the filaments must be higher than the pressure required to extrude the filaments through the nozzle tip. PU is categorised as a soft or flexible material prone to buckling. The addition of the fillers like particles or fibres could enhance its elastic modulus and buckling resistance so that it may improve PU printability [67].

A model may be used to predict the coalescence behaviour of composites achieved by using SLS technique [68]. In this case, a low viscosity of the feedstock material for SLS printing from polymers is required to achieve adequate coalescence between polymer particles since SLS machine cannot provide an additional compacting during a printing process [117]. High viscosity causes insufficient liquidity and inappropriate coalescence [118]. Coalescence behaviour of PU/CNT powders during SLS printing can be described by Frenkel's sintering model [119] according to equation (9).

$$\left(\frac{x}{R}\right)^2 = \frac{3}{2\pi}\frac{\sigma}{R\eta}t \tag{9}$$

R, x, σ, η and t are the particle radius, neck radius formed between two particles, surface tension, melt viscosity and sintering time. Such a simple model indicates that the viscosity plays a crucial role in material sinterability.

4. SMPU composites for 4D printing

4D printing refers to the ability of 3D printed materials to actuate when a stimulus such as a temperature, electricity, light, pressure or moisture is applied [120]. The particular materials used for 4D printing must possess shape memory properties enabling them to remember and recover their original shape. It means an external force can deform the original shape of shape-memory materials into a temporary form. This temporary form is retained until a stimulus is applied, which triggers the transformation of shape-memory materials to return their original shape [121,122]. Shape-memory materials can perform such a unique action due to the presence of elastic and transition segment [123], making these materials recover their shape under the effect of an appropriate stimulus after being physically deformed [124].

A shape-memory material like SMPU could be a promising candidate for several applications such as scaffolds, sensors, actuators, wearable and biomedical devices [19,60,65,70]. However, pristine SMPU properties have not met the requirements of final products yet. Hence, it should be combined with other materials like polymers and fillers so as to greatly improve its properties. The addition of fillers in SMPU matrix may improve shape memory feature, electrical property, sensing capability, biocompatibility and self-healing. The use of additional fillers like CNTs, carbon black (CB), PCL and WF can be conducted using solution and melt mixing [125–128]. Table 6 lists generally used SMPU materials and their composites particularly with respect to 4D printing in detail.

Most of SMPU composites are processed using FDM technique due to its ability to handle various materials, as well as composites such as SMPU/MWCNT nanocomposites, SMPU/CB nanocomposites and SMPU/tungsten nanocomposites [125,126,129]. Besides, this technique also offers low-cost manufacturing compared to other 3D printing methods like PolyJet technology [78]. Nevertheless, FDM has typical drawbacks by producing printed parts with worse surface finish, less dimensional accuracy, as opposed to those printed by PolyJet technology [125].

4.1. Preparation of SMPU composites for 4D printing

The preparation of SMPU composites is similar to that of PU composites for 3D printing. Purification, dehumidification and mixing processes are required to produce feedstock materials for 4D printing. A summary of 4D printing applied to process SMPU composites along with the associated stimuli and programming process is listed in Table 7.

The reinforcement materials for SMPU typically comprise particles, nanoparticles and polymers that can be easily mixed with polymer matrix via solution or melt mixing [60,80,125–130]. In FDM technique, SMPU and the reinforcements should be processed in form of 3D filaments using a filament extruder. This extrusion process must take into account the melting temperature (T_m) of raw materials, primarily shape memory properties under material processing particularly for SMPU. Otherwise, it may damage the prepared filaments, or yield the filaments with inconsistent diameter sizes or rough surfaces. This state also applies to the extrusion process in 3D printing. To produce the desired printed parts, nozzle temperature must be selected in reference to the T_m of materials, and the other printing parameters, namely print speed, layer height, and filling ratio of 3D printer should also adapt to filament properties [125].

4D printing often uses thermoplastic polyurethane (TPU) since it possesses excellent shape memory behaviour. TPU belongs to the family of PU materials with many different grades. The most common TPU with shape memory properties are TPU elastomer, polyester and polyether grades. Based on the database of MatWeb [131], the T_m of TPU elastomer, polyester and polyether grades are in the range of 100–230°C, 71-221°C and 118-218°C, respectively. Therefore, the nozzle temperature for the printing process is commonly set in the range of 200–240°C [60,125,130].

The programming process in 4D printing for SMPU that applies heat as external stimulus must refer to its T_g (a critical transitional temperature taking place between glassy and rubbery state). Therefore, deformation program should be performed above this temperature level. For instance, when TPU has the T_g of 35°C, printed structures should be heated above this temperature (e.g. 40°C) [125]. If its T_g is 55°C, programming temperature is recommended being adjusted to 75°C [130]. Besides, TPU is also known as a flexible material with low stiffness due to its own large elongation by means that this material is susceptible to buckling when subjected to a printing process. If print speed is too high, extruded filament diameter through the nozzle tip decreases resulting in lower critical buckling pressure (P_{cr}) [132]. If P_{cr} is lower than the pressure required to extrude the filaments, it induces the buckling on the filaments (see equation (8)). Hence, the used printing speed for 3D printing techniques such as FDM cannot be too high in range of 20–80 mm s^{-1} [126,129] to maintain a consistent flow of deposited filaments.

4.2. Properties of 4D printed SMPU composites

Printing parameters such as printing temperature, feed rate, filling ratio and layer thickness can influence the properties of 4D printed SMPU composites. Ly et al. [125] investigated the effect of such four printing parameters on the conductivity and recovery behaviours of SMPU/MWCNT composite samples using FDM. This study revealed that the recovering time of composite samples significantly declined when the stimulus temperature was higher than their T_g. It is noteworthy that for an effective recovering time, the stimulus temperature applied should not exceed 10°C below T_g [125].

The printing parameters of FDM technique affected electrical resistance and recovering time of SMPU/MWCNT nanocomposite samples [125]. Compared with samples in the same printing parameter category, one that possesses either higher printing temperature, layer thickness, filling ratio or lower feed rate yields lower electrical resistance and shorter recovering time. The difference in printing temperature and layer thickness contributed to the greatest effect on recovering time [125]. High printing temperature can easily bond layers together into a thicker one containing more MWCNTs, leading to enhanced electrical conductivity. High filling ratio and low feed rate induced the same effect on depositing MWCNTs into layers. The best performance of composite samples with the resistance and recovering time of 0.95 kOhm and 42 s

Table 7
Summary of 4D printing for SMPU composites.

Method	Matrix material	Reinforcement	Material preparation process	Printing parameter	Stimulus	Programming process	Ref.
FDM	TPU with T_g of 35°C	MWCNT	• Solution mixing • Ultrasonication • Stirring • Vaporisation • Shredding • Drying • Melt mixing • Extrusion	• Print speed: 40 mm/s • Nozzle temperature: 200°C • Bed temperature: 70°C	Heat	• Heating the sample above their T_g (40°C) • Applying external force to deform the sample • Maintaining this deformation at below T_g (20°C) • Releasing the applied force • Immersing the samples into water at 40, 45, and 50°C	[125]
FDM	TPU with T_g of 45°C	CB	• Solution mixing • Sonication • Evaporation • Cutting • Melt mixing • Extrusion	• Print speed: 80 mm/s • Nozzle temperature: 230°C • Bed temperature: 60°C • Layer height: 0.25 mm • Infill: 100%	Electrical current	• Applying external force and electrical current to deform the samples up to their ultimate tensile strength • Maintaining this deformation • Releasing the applied force and turn off the electrical current after the sample reaches its fracture point	[126]
FDM	TPU with T_g of 35°C	Tungsten	• Ball milling • Solution mixing • Stirring • Drying • Melt mixing • Extrusion	• Print speed: 20 mm/s • Nozzle temperature: 230°C • Bed temperature: 55°C • Layer height: 0.2 mm • Infill: 100%	Heat	• Heating the sample above their T_g (60°C) • Compressing the sample until it is deformed up to ½ of its thickness • Maintaining this deformation and the sample is cooled at -10°C • Releasing the applied force • Immersing into water at 40°C	[129]
FDM	TPU with T_g of 55°C	Nylon	Extrusion	• Print speed: 50 mm/s • Nozzle temperature: 230°C •Bed temperature: 25°C • Layer height: 0.2 mm • Infill: 100%	Heat	• Heating the sample at 70°C for 5 min • Deforming the object shape • Cooling the sample for 30 min • Reheating the sample at 70°C for 5 min	[130]
FDM	TPU with melting temperature (T_m) of 170–220°C	• PCL • MWCNT	• Solution mixing • Stirring • Washing • Drying • Creating composite films • Crushing the composite films • Extrusion	• Print speed: 30 mm/s • Nozzle temperature: 230°C • Bed temperature: 30°C • Layer height: 0.4 mm • Infill: 100%	Light (near infrared)	• Heating the sample above $T_{m\text{-}PCL}$ • Deforming the object shape • Cooling the sample • Applying near infrared (NIR) to reheat the sample	[127]
FDM		• WF	• Mechanical mixing		Heat	• Heating the sample above $T_{m\text{-}TPU}$ for 2h	[128]

(*continued on next page*)

Table 7 (*continued*)

Method	Matrix material	Reinforcement	Material preparation process	Printing parameter	Stimulus	Programming process	Ref.
	TPU with T_g of −20°C		• Melt mixing • Extrusion	• Print speed: 25 mm/s • Nozzle temperature: 230°C • Bed temperature: 30°C • Layer height: 0.2 mm • Infill: 100% • Filling angle: 45°		• Deforming the sample • Cooling the sample at −25°C for 12 h • Reheating the sample above $T_{m\text{-}TPU}$	
FDM	TPU filament	• PLA filament with T_g of 60–65°C	• Cutting the filament to the pellet rods • Aeration with the compressed air • Melt mixing • Extrusion	• Print speed: 10 mm/s • Nozzle temperature: 240°C • Bed temperature: 70°C • Layer height: 0.3 mm	Heat	• Heating the sample at 70°C • Stretching the sample • Cooling the sample at 21°C for 5 min • Reheating the sample at 70°C	[60]
Modified FDM	Waterborne PU	• Carbomethyl cellulose (CMC) • Silicon dioxide (SiO_2)	• FDM modification (the FDM nozzle was replaced by a syringe) • Solution mixing • Stirring • Extrusion	• Pump pressure: 3–50 psi • Layer height: 0.5–0.7 mm • Bed temperature: 50°C	Heat	• Heating the printed object at 121°C onto a hot plate • Deforming the object to a new shape • Removing object from the hot plate • Placing the object onto the hot plate at 121°C	[80]

accordingly, were obtained when printing temperature, feed rate, filling ratio and layer thickness were set to be 230°C, 40 mm s^{-1}, 100%, and 0.2 mm, respectively [125].

Important properties of printed SMPU composites such as toughness, elongation and electrical conductivity can be improved by incorporating CB particles in SMPU matrix. Rosales et al. [126] varied the CB contents of 1, 3, 5, and 7 wt% and mixed it with SMPU and N-dimethylformamide (DMF) solvent by using the solution and melt mixing method. Besides, the electrical current was employed as an external stimulus instead of heat. In general, increasing the CB content promoted the electrical conductivity of SMPU/CB composites. Optimally, it reached the best performance with the inclusion of 5 wt% CB. Nevertheless, composite filaments reinforced with 1 and 3 wt% CB lost the conductivity properties. It could be related to nanocomposite mixing conditions at a low temperature (i.e., 160°C) and a low pressure (approximately 0.32 MPa) since the filament extruder employed in this study was a single-screw type containing a single heating chamber. The printed composite samples reinforced with 5 and 7 wt% CB exhibited better electrical conductivity than those with the addition of 1 and 3 wt% CB (i.e. 0.1822 × 10^{-3} and 3.83 × 10^{-3} S m^{-1}, respectively) [126]. However, SMPU/CB composite filaments containing 5 wt% CB appeared to be too soft and caused material clogging issue in the nozzle tip during deposition. In contrast, composite samples reinforced with 7 wt% CB became too brittle and induced high breaking rate during the extrusion process. To overcome the stiffness issue, an additional master batch of composites containing 7 wt% CB was manufactured. They were then mixed with SMPU (weight ratio: 1:0.33) in the filament extruder to create composite filaments reinforced with 5 wt% CB. The presence of electrical stimulus assisted successfully in enhancing the toughness of composite samples up to 4 times higher as opposed to controlled samples, and elongation was improved from 9.45 to 44% on the same basis [126]. It reflected the superplastic properties of nanocomposite samples when an electrical stimulus was employed throughout the programming duration.

Other particles, namely tungsten can be used as the reinforcement in SMPU matrix to increase shape holding and shape recovery of printed composite structures. Kashyap et al. [129] combined SMPU with Tungsten and sodium chloride (NaCl) to produce porous radiopaque in possession of shape memory property for endovascular embolisation. The shape recovery of composite samples reached 95% during the first recovery cycle, and then increased up to 100% at the next recovery cycles [129]. It was evidently confirmed that porous Tungsten SMPU exhibited a remarkable shape holding and shape recovery properties. However, the storage modulus of porous SMPU/Tungsten composites was lower than that of moulded SMPU, but it was still 12% higher than that of porous SMPU.

Other factors such as thickness and cycles also impact shape memory and tensile properties of sinusoidal nylon/SMPU composite structures via FDM [130]. This study disclosed that the sinusoidal pattern resembling an oscillating wave could achieve excellent mechanical properties [133]. Besides, it used five different thicknesses in the sinusoidal pattern, namely 0.2, 0.4, 0.6, 0.8, and 1.0 mm subjected to the printing on nylon fabric with sample codes of 0.2, 0.4, 0.6, 0.8, and 1.0 SM/NF, respectively (Fig. 25).

The thinner sample could recover faster than the thicker counterparts. As shown in Fig. 26, those samples with a thickness of 0.2 mm (0.2 SM/NF) had the highest shape recovery rate, which was followed by 0.4, 0.6, 0.8 and 1.0 SM/NF. The average shape recovery rates during 50 cycles were 3.0, 2.0, 1.4, 0.8 and 0.7°/s for 0.2, 0.4, 0.6, 0.8 and 1.0 SM/NF, respectively. The higher printing thickness yielded more layers so that it required more time for heat transfer from the exterior to internal layers. Conversely, the thinner samples took less time to transfer heat to the entire region of the samples in order to reach T_g and shift to the rubbery state. Therefore, it could release the stored force and recover quickly [134]. The curve patterns in Fig. 26 confirmed that the shape recovery rate declined with increasing sample thickness.

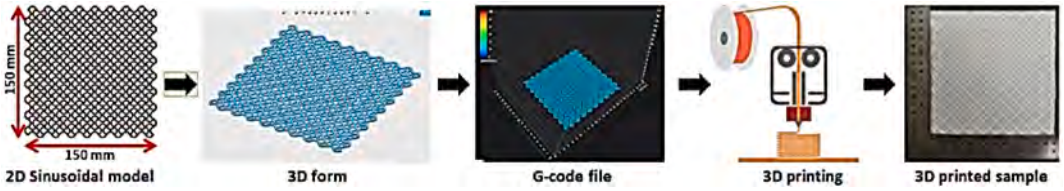

Fig. 25. Sinusoidal nylon/SMPU composite samples [130].

4.3. Shape-memory effect (SME), stimuli and associated mechanisms

The SMPU possesses two microphase-separated structures because of thermodynamic incompatibility between hard and soft segments. The hard segment is made from diisocyanate and chain extender while the soft segment comes from the long-chain polyol. This hard segment may bind itself via hydrogen bonding and crystallisation, and it makes SMPU become very solid below its T_m. Reversible transformation of soft segments is believed to be responsible for SME of the material. To investigate SME, several testing methods such as tension, compression, flexural, relaxation and creep tests may be applicable for this purpose [135,136].

SME, stimuli and particular mechanisms should be involved when study material shape memory properties such as SMPU. Kashyap et al. [129] applied heat as an external stimulus to actuate SME of SMPU. This study included programming and recovery steps to investigate the shape memory behaviour of SMPU/Tungsten composite samples in size of 10 mm × 10 mm × 10 mm. Firstly, This sample was heated in an oven at 60°C with reference to the T_g of SMPU (i.e. 35°C). The composite sample was then compressed to a thickness of 5 mm in one of its dimensions and cooled at −10°C in a freezer to fix its temporary shape. The recovery step was conducted by immersing the sample in a water bath at 40°C until it achieved full shape recovery. The dimensions of composite samples in the compression direction were measured to evaluate its shape recovery. The shape recovery process of the composite sample is shown in Fig. 27.

Another stimulus, namely electrical current, was applied to investigate toughing improvement of SMPU/CB nanocomposite structures during a programming process [126]. The material samples were fabricated in a dog-bone form according to ASTM standard D638 type IV. The applied mechanism in this research to study shape memory effect of printed composites was a combination of the tensile-test procedure with electrical current supply. It started at room temperature, which was below the T_g of SMPU material at 45°C. Whereas the electric current from DC power supply with an output capacity of 300 V was applied through the sample during the elastic deformation region. This power supply was turned on and off at the particular time in the tensile tests. When the sample reached the fracture point, the load was entirely removed [126].

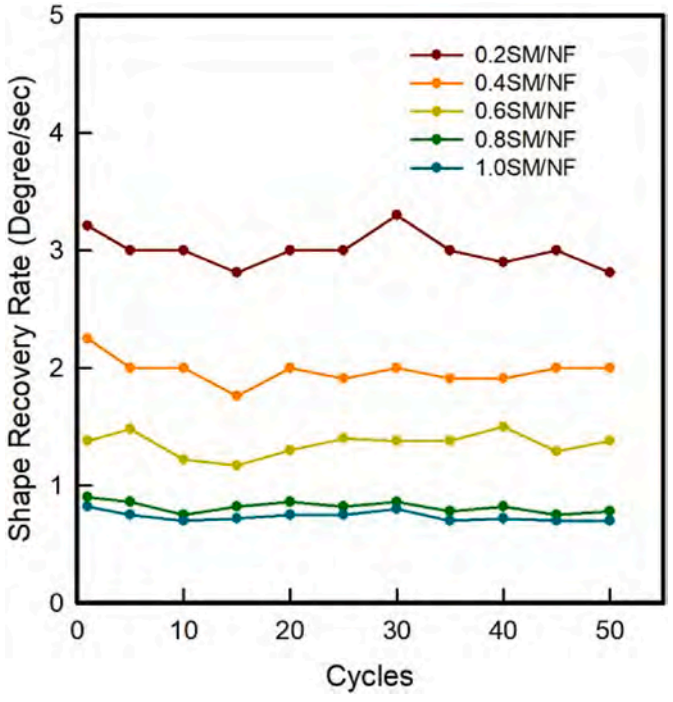

Fig. 26. Shape recovery rate of nylon/SMPU composite samples with various thicknesses and cycles [130].

The near-infrared (NIR) light was imposed by Bi et al. [127] to activate SME of dopamine-modified SMPU/PCL/MWCNT composite samples manufactured by FDM. The incorporation of MWCNTs was supposed to absorb NIR light and convert it into heat so that it enabled to increase the temperature of composite samples and to remotely control localised shape change [33,132]. However, the interaction between these nanoparticles and polymer matrix is weak, and the van der Waals force between those particles is conversely strong leading to typical particle aggregation. Therefore, the surface modification of fillers is necessary to improve the interfacial interaction between nanoparticles and polymer matrix. The preparation of feedstock material for FDM technique can be conducted via solution and melt mixing methods.

The shape memory mechanism of SMPU/PCL/MWCNT composite samples induced by the NIR light is similar to that being triggered by heat. The difference is that MWCNTs are used as the photothermal conversion materials while NIR is employed as the light source [127]. The programming process to observe SME of composite samples is illustrated in Fig. 28. In this process, when the temperature condition is lower than the T_m of PCL, PCL molecular chains are frozen in a solid state because of its low molecular movement and crystallisation. Once the temperature is higher than the T_m of PCL, PCL crystals become quite soft, and polymeric chains may undergo a significant segment movement in order to change polymeric structures. In the temporarily deformed state, PCL in the composite structure is in a crystalline state with a deformed shape. When the NIR light is imposed, the composite temperature exceeds the T_m of PCL via the photothermal effect of MWCNTs. It can also soften PCL crystals due to the elastic effect of SMPU so that the composite shape is gradually recovered and return to its initial shape. In this composite material system, high crystallinity and ductility of PCL region determine its fixed shape ratio. On the other hand, the elastic SMPU region stores the deformation energy that is released during the heating process, softens and restores the shape of PCL crystals [137–139].

5. Applications

One of 3D printing superiorities, when compared to conventional methods such as injection moulding, is its capability to manufacture a complex geometry structure. This superiority allows 3D printing to fabricate various structures such as flexible sensors, scaffolds, finger orthosis, thermoelectric generator and wearable devices made from PU composites [19,58,65,68,92].

Smart PU ability, to be deformed and recover its original shape when triggered by external stimuli such as light, heat and electrical current, is the unique characteristics of this material [140]. It is supported by the presence of microphase-separated domains (i.e. hard and soft segments).

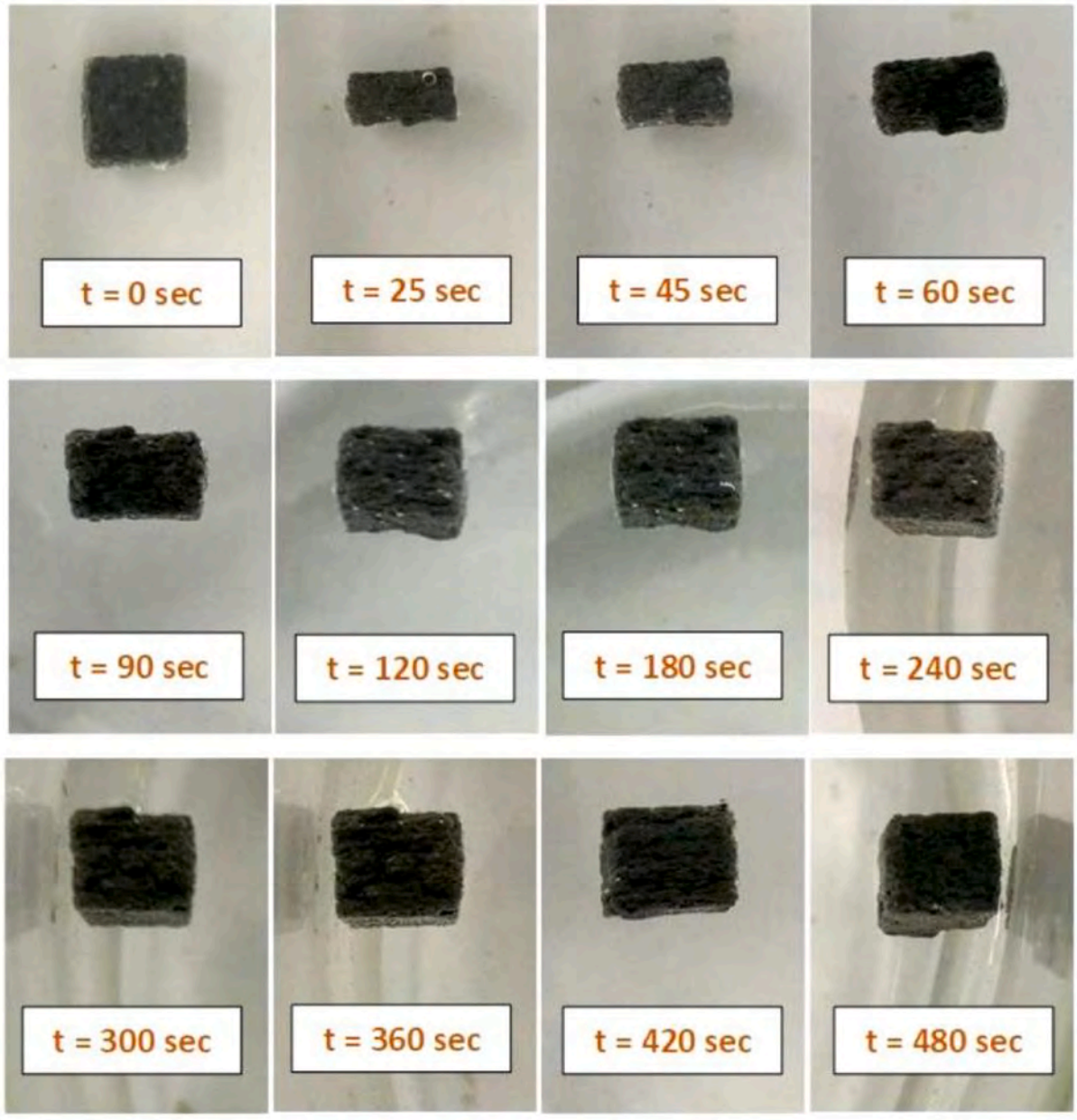

Fig. 27. The shape recovery process of SMPU/Tungsten composite sample [129].

The hard segments supply the mechanical strength to remember initial shape after deformation while dissipation energy is stored by soft segments which are used for returning to the original form under external stimuli [141]. The SME in PU and its composites could be one-way, two-way, triple, or even quadruple depending on the number of transition temperatures and the content of hard and soft segments

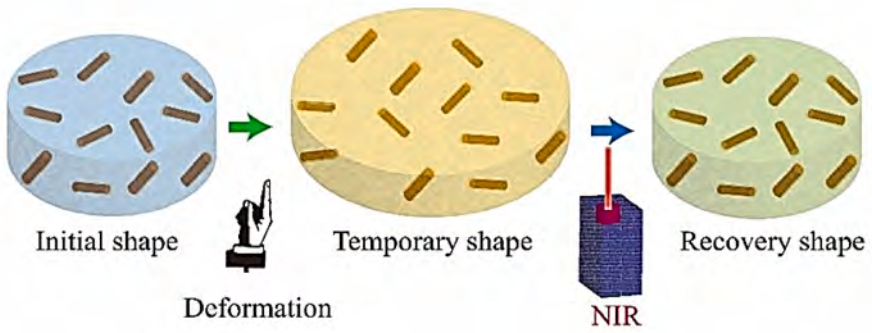

Fig. 28. The process of NIR-induced SME in dopamine-modified SMPU/PCL/MWCNT composite sample [127].

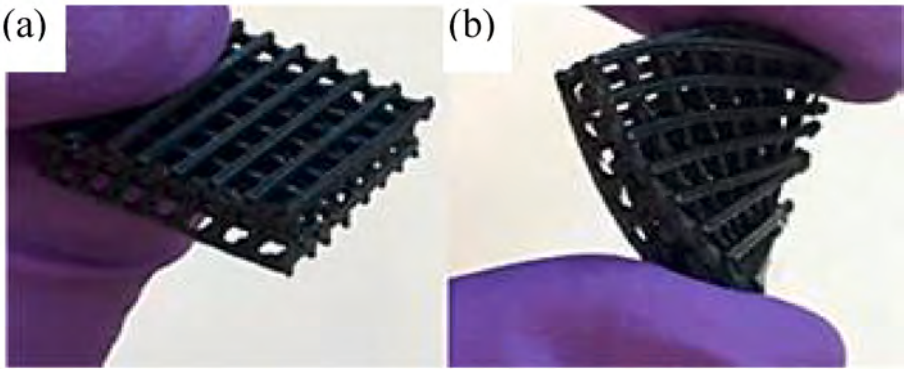

Fig. 29. (a) 3D printed PU/PLA/GO nanocomposite scaffold and (b) 3D printed PU/PLA/GO nanocomposite scaffold under bending. Adapted with permission from Ref. [19]. Copyright 2017 American Chemical Society.

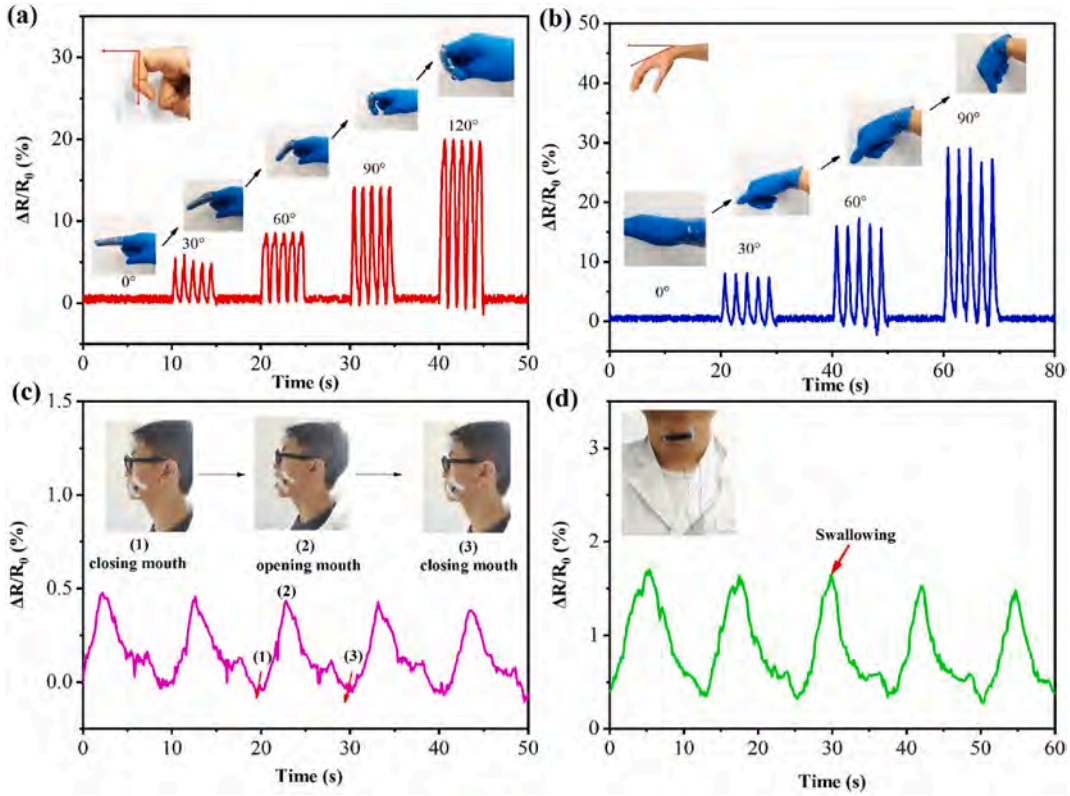

Fig. 30. Electromechanical sensors based on TPU/MWCNT/AgNP nanocomposites for repeated bending and unbending based on (a) index finger, (b) wrist, (c) mouth opening and (d) swallowing [67].

[142–144]. The ability of smart PU makes this material become a strong material candidate for a wide range of applications such as flexible sensors, smart structures for tissue engineering and biomimicking skeletal muscle actuator [60,80,128].

5.1. Biomedical applications

Millions of reconstructive surgical procedures are performed yearly to overcome bone injuries due to the annihilation of bone tissues such as osteoporosis, tumours and osteonecrosis [145]. The destruction of bone tissues could be caused by traumatic injuries or ineffective healing after traumatic injuries. Typically, a human body heals the bone fracture using different bone cells to start with bleeding. When the blood flows down to the site of bone fracture, it forms a clot inducing swelling in the broken area. The healing process time for every person may differ depending on the health condition, age, the presence of infection, breakage type and blood supply condition [140]. A small defect in the bones may be healed naturally through growth, renewal and repair mechanisms. Nevertheless, when a bone defect is bigger than the critical size, the healing process becomes crucial with the requirement of a bone regeneration method based on tissue engineering techniques. A scaffold can be categorised as the most important part in tissue engineering to regenerate target tissues such as bone defects.

The process of scaffold design and its implantation in human bodies requires precisely matched dimensions with the bone defect contour. Regarding this, smart PU composites with shape memory properties may make a significant contribution. These properties allow smart PU composites to maintain a temporary programmed shape and recover as per

Table 8
Applications and challenges of smart PU for 3D or 4D printing in biomedical engineering.

Method	Materials	Application	Challenges	Ref.
FDM	TPU/hBN	Sensor	The printed samples have anisotropic properties from hBN filler	[64]
FDM	TPU/MWCNT	Flexible sensor	The printed samples inherit the piezoresistivity anisotropy	[65]
FDM	TPU/MWCNT/AgNP	Flexible sensor	Without the presence of AgNP, the numerous CNT agglomeration in the TPU matrix occurred that lower the sensitivity and linearity of the printed composites	[67]
FDM	TPU/PLA/GO	Scaffold for tissue engineering	The printing orientation influences different mechanical response because of the weak adhesion strength between layers during printing process	[19]
FDM	TPU/PLA	Finger orthosis	The single-screw extruder requires three times of melt mixing process leading to time-consuming manufacturing	[90]
FDM	SMPU/Tungsten/NaCl	Interventional radiology	It is arduous to print SMPU possessing a low Tg (35°C) since it loses its stiffness at room temperature	[129]
FDM	• SMPU waterborne/ carbomethyl cellulose (CMC) • SMPU waterborne/silicon dioxide (SiO_2)	Smart structures for tissue engineering	• The addition of CMC and SiO_2 decreases the fracture stains of the samples • The printed objects still have rough forms (poor accuracy) • The printing process is time-consuming since it requires 1–2 min delay between each layer	[80]
FDM	SMPU/PLA	Biomimicking skeletal muscle actuator	• The printed actuators have low durability • Response time is still too long	[60]
DIW	PU/HA/Y27632 or TGFβ3	Scaffolds	The bulk structure of PU/hyaluronan (HA) scaffolds disintegrate after one month due to low solid content	[17]
SLS	TPU/CNT	Wearable devices	The increasing CNT content decreases the tensile strength of the composite samples due to the incomplete coalescence of polymer particles	[68]
DLP	• PU/polyaniline (PANI) • PU/graphene sheet (GS)	Biomedical devices	The effect of PANI addition to tensile strength and Young's modulus of the composite samples is not significant	[70]
SLA	PU/PLA/graphene/TE GDMA	Scaffolds	SLA technique generates anisotropic property on the printed composite structures	[18]

requirement after the incorporation in a bone through minimal invasive bone repair [146]. Chen et al. [19] used PU, PLA and GO nanoparticles to produce a nanocomposite scaffold, as illustrated in Fig. 29, with the aid of FDM. The combination of those materials was found to increase mechanical strength and thermal stability of the scaffolds. Besides, these scaffolds showed good biocompatibility with NIH3T3 cells, indicating their critical role as potential biomaterial scaffolds for tissue engineering. However, the printing orientation affected the mechanical response of composite scaffolds due to weak adhesion between layers during the printing process, which is deemed as a typical drawback to FDM technique.

Smart PU composites may also be used to produce a flexible sensor for prosthetics. CNT particles are typically utilised to reinforce PU or SMPU matrix. Kim et al. [65] combined the TPU and MWCNTs to create a flexible pressure sensor using FDM. The piezoresistivity of flexible sensors with an MWCNT content of 5 wt% was characterised using tensile tests up to 40% strain, which were conducted parallel to the loading and transverse directions, and simultaneously measured the resistance of sensors. The results revealed that the isotropy of resistivity was maintained during deformation [65]. Another similar work had been conducted by Xiang et al. [67] that manufactured elastic strain sensors using FDM by combining TPU, MWCNTs and silver nanoparticles (AgNPs). The incorporation of nanofillers improved material printability and significantly affected the sensing performance of nanocomposite sensors. The electromechanical responses of nanocomposite sensors are shown in Fig. 30. When the weight ratio between MWCNTs and AgNPs was 5:1, the sensors possessed high sensitivity (gauge factor (GF) = 43260 at 250% strain), fast response (~57 ms), high linearity ($R^2 = 0.97$ within 50% strain), and excellent repeatability (1000 cycles) owing to synergistic effects [67]. These results indicated the sensor potential for specific applications in prosthetics and wearable devices where customisability is typically required.

The combination between TPU and PLA results in excellent properties such as flexibility, biocompatibility and fixity particularly required by wearable devices for biomedical applications such as skeletal muscle actuators and finger orthosis [60,90]. A skeletal muscle actuator is used to facilitate the movement and force to joints within a prosthetic device. For upper limb prosthetic, it involves digit/wrist manipulation, rotation at the elbow and grip force. Therefore, it needs an actuator that can provide a linear output or translate rotational energy to a linear force/direction. Current prosthetics for upper limb amputations uses a body-powered system or an electric system. Nevertheless, both systems have drawbacks. The body-powered system has no feedback system or high force output but appears to be lightweight and inexpensive along with a lack of complexity. Whereas the electric system is more costly and heavier resulting in noise pollution. Nonetheless, it has a feedback/-control system enabling to collect the input from the electrodes of muscular monitoring [60,147,148]. The printed TPU/PLA composites fabricated by FDM have been developed to overcome such disadvantages. Shape memory property possessed by TPU and PLA allowed the actuator to memorise a predetermined shape and recovered to the initial shape when a stimulus like the heat was applied. The printed composite actuator demonstrated nonlinear properties in which strain and peak force were comparable with those of mammalian skeletal muscle. This actuator had the response time of 0.77s, low mass of 74.0 mg, low operating temperature at 70°C and material cost of US$0.0098 per actuator [60]. However, this actuator may have an issue related to durability and loading protection within a prosthetic.

The finger orthosis derived from TPU/PLA composites via FDM was implemented by Tao et al. [90]. This work revealed that TP25 specimens, consisting of 25 wt% TPU and 75 wt% PLA, exhibited the same tensile strength, but higher elongation at break than neat PLA. It indicated that the printed TPU/PLA composites with such a composition could meet material requirements of finger orthosis. However, a further increase of TPU up to 50 wt% leads to a sharp decrease in the tensile strength of printed composite structures [90]. A summary of applications and challenges of smart PU used for 3D or 4D printing in biomedical engineering is presented in Table 8.

5.2. Electronics applications

3D printing technology has been widely used in the fabrication of electronic parts or devices since it can yield appropriate geometry with reduced time when compared with traditional manufacturing such as injection moulding [149]. When this technology is combined with smart PU composites, it can produce various electronic components, namely sensors, flexible circuits, wearable devices, soft robotics and thermoelectric generators, as mentioned earlier by Tzounis et al. [58]. This

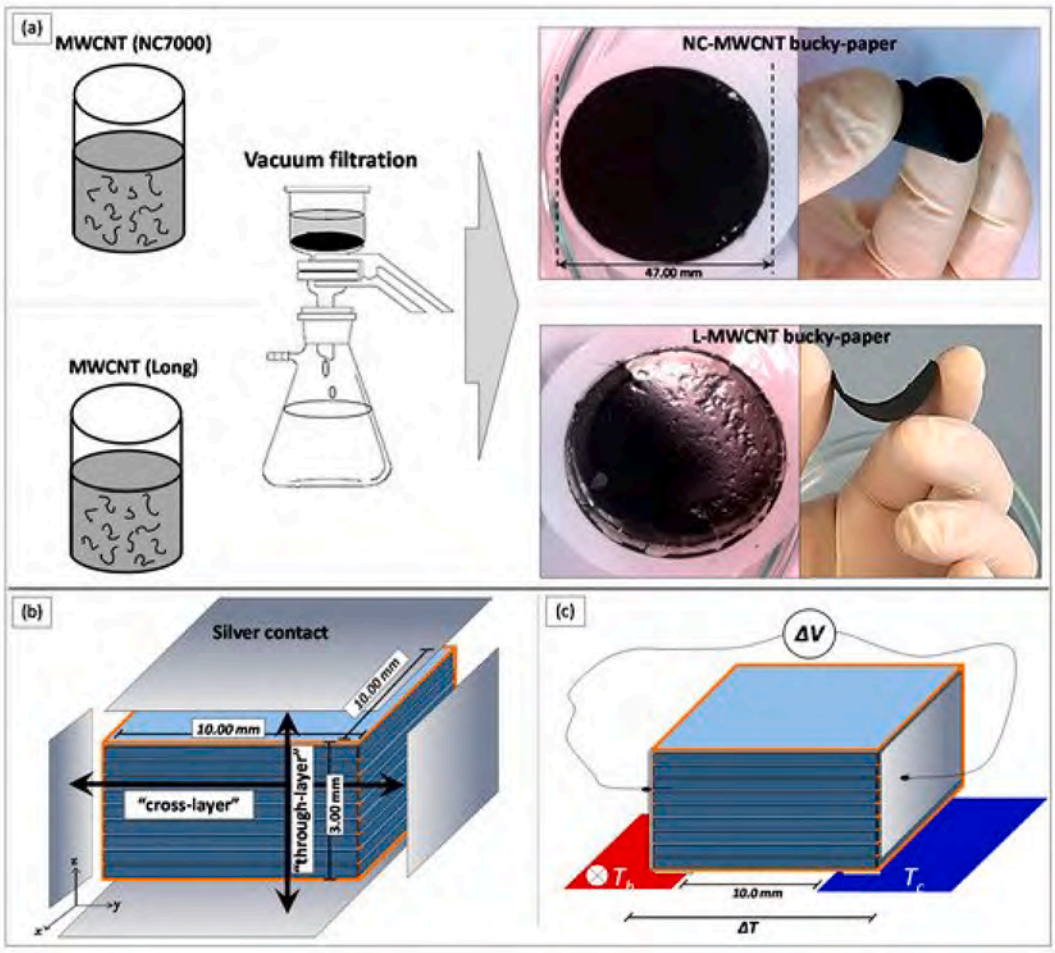

Fig. 31. (a) Vacuum filtration process to create MWCNT bulky paper films, (b) schematic diagram of cross-layer and through-layer electrical conductivity measurements and (c) thermal gradient set-up used for Seebeck coefficient measurements [58].

study manufactured a flexible and stretchable organic thermoelectric device from TPU and two types of MWCNTs, namely NC-7000 MWCNTs, called NC-MWCNT, and Long MWCNTs, known as L-MWCNT using FDM (Fig. 31). Thermoelectric device has the ability to generate an electric potential, which is known as thermoelectric voltage, upon being exposed by heat. Even though printed samples showed an anisotropic electrical conductivity in the printing direction of through-layer and cross-layer, it yielded the same Seebeck coefficient [150]. This result may unravel an opportunity for the 3D printed thermoelectric TPU/MWCNT nanocomposites toward large-scale thermal energy-harvesting applications such as stretchable 3D harvester and wearable devices with the requirements of complex geometry and customisability.

In addition to thermoelectric devices, the combination of PU and MWCNTs are also applicable to create strain, flexible or piezoresistive sensors. Christ et al. [26] employed both materials to manufacture uniaxial and biaxial strain sensors using FDM. Such sensors underwent a series of cyclic strain loads to investigate their piezoresistive responses. The results indicated that TPU/MWCNT nanocomposite sensors achieved excellent responses with cyclic repeatability in both axial and transverse directions, as well as in response to strains as high as 50% [26]. It demonstrated the possibility of fabricating embedded and multidirectional flexible strain sensors using 3D printing along with potential applications in flexible electronics, health monitoring and soft robotics. A sensor possessing excellent elastic and electro-responsive properties may be made from SMPU/CB composites via FDM [126]. The primary challenge in sensor manufacturing was associated with increasing composite brittleness due to the addition of CB nanoparticles so that it triggered a premature breaking under tensile loads. Such a drawback was tackled by increasing the sample temperature to pass a controlled current through the part in order to tailor its strength properties. The results showed that conductive SMPU/CB nanocomposite samples responded to electrical current stimulus by enhancing their toughness four times higher than that without the current applied during the tensile tests. However, as previously predicted, the inclusion of CB nanoparticles in SMPU matrix diminished the elongation of composites by approximately 50%, as opposed to that of pristine SMPU [126]. It might be ascribed to the reduction in interfacial interaction between polymeric chains due to the CB dispersion within polymer matrix.

The sustainability of smart PU composites should be considered since this kind of material has good potential applications in several areas such as biomedical engineering and electronics. It can be achieved by using biomass materials like WF with abundance, low cost, low density and environmental friendliness [63]. The combination of SMPU and WF must be followed by the addition of ethylene- propylene- diene-monomer grafted maleic anhydride (EPDM-g-MAH) as a modifier in order to compensate for the loss of toughness and enhance the interfacial adhesion of SMPU/WF composites [63]. Bi et al. [128] used SMPU, WF and EPDM-g-MAH to fabricate composite samples in possession of good shape memory property, tensile strength and tensile elongation. The experimental results revealed that when the EPDM-g-MAH content was 4 wt%, well-dispersed WF particles in the composites with strong interfacial bonding between SMPU and WF were obtained. Besides, a better recovery ratio was also achieved at this composition when

Table 9
Applications and challenges of 3D or 4D printing of smart PU in electronics.

Method	Materials	Application	Challenges	Ref.
FDM	TPU/MWCNT	Stretchable organic thermoelectric generator	The printed samples exhibited an anisotropic electrical conductivity	[58]
FDM	TPU/MWCNT	Strain sensor	The transverse sensor response was much lower than what was demonstrated by the axial sensor	[26]
FDM	TPU/MWCNT	Sensor	The stress-strain relationship may vary significantly when repeatedly loaded to large strain	[62]
FDM	TPU/MWCNT	Flexible sensor	The printed samples inherited the piezoresistivity anisotropy	[65]
FDM	TPU/MWCNT/ AgNP	Flexible sensor	Without the presence of AgNP, the numerous CNT agglomeration in the TPU matrix occurred that lowered the sensitivity and linearity of the printed composites	[67]
FDM	TPU/hBN	Sensor	The printed samples inherited anisotropic properties from hBN filler	[64]
FDM	SMPU/MWCNT	Sensor	Technical issues, such as material clogging, frequently occurred so that it consumed much time and labour	[125]
FDM	SMPU/CB	Sensor	The incorporation of CB decreased the composite elongation up to 50%	[126]
FDM	SMPU/WF/EPDM-g-MAH	Soft robotics, flexible electronics, sensors	The increasing content of ethylene- propylene- diene- monomer grafted maleic anhydride (EPDM- g-MAH) over 4% lowered both tensile strength and elongation of the printed samples	[128]
SLS	TPU/CNT	Flexible circuit, wearable devices	The increasing of CNT content decreased the tensile strength of the composite samples due to the incomplete coalescence of polymer particles	[68]
SLS	TPU/SWCNT	Flexible piezoresistive sensor	The increasing of SWCNT content declined the tensile strength	[69]
DLP	• PU/polyaniline (PANI) • PU/graphene sheet (GS)	Antistatic materials, sensors	The effect of PANI addition to tensile strength and Young's modulus of the composite samples was not significant	[70]

compared to that based on unmodified- SMPU/WF composites [63]. This finding revealed a great potential of SMPU/WF composites for soft robotics, sensors and flexible electronics. A summary of 3D or 4D printing applications for smart PU in electronics with their major challenges is indicated in Table 9.

When compared to other 3D techniques, FDM is used more frequently to handle smart PU and its composites. It may be caused by FDM superiorities that can process various kinds of materials, which is thus classified as low-cost manufacturing with user-friendliness [125]. However, this technique has some drawbacks, as indicated in Table 9. The printed composites resulted in anisotropic properties arising from FDM process [58,64,65] due to its nature. It could be improved by means of post-processing such as post-heating process. Other disadvantages of FDM technique are material agglomeration and clogging [125], as well as filament buckling [114]. The agglomeration issue may be tackled using an appropriate mixing method for raw materials so that the fillers can be well distributed in the matrix. The modifiers such as EPDM-g-MAH and MDI can be proposed to enhance interfacial adhesion between the fillers and the matrix [20,80,129,130] since it is allowed to strengthen the particle bonding in composite laminates and improve the mechanical strength of printed structures. Filament buckling problem could be solved by increasing the filler content to enhance filament elastic modulus [62]. However, when the filament is too stiff, it may induce material clogging in the nozzle.

The addition of the reinforcements does not always induce significant effect on the matrix properties, as evidenced by the incorporation of PANI in PU matrix [70]. Furthermore, increasing the filler content up to a certain level may worsen the tensile strength due to the incomplete coalescence of polymer particles or agglomeration [68,69,90]. Therefore, the optimal composition between the matrix and fillers should be determined accordingly in order to achieve the desired properties.

6. Summary and future challenges

SMPU consists of two microphases, namely hard and soft segments. The hard microphase imparts the stiffness and offers the reinforcements to the material while the soft microphase contributes to elastic behaviour. Such a unique characteristic generates SME in smart PU structures under either external force or stimuli. It allows this material and its composites to be used for general purpose such as scaffolds, flexible sensors, finger orthosis and wearable devices in biomedical engineering and electronic fields. The fabrication process of those products involves 3D printing techniques such as FDM, DIW, SLS and DLP. The 3D printing technology becomes an alternative way to create objects with complex geometries, which is arduous to be performed by traditional manufacturing methods, namely extrusion, compression moulding and injection moulding.

The sustainability of smart PU refers to renewable raw materials to replace traditional petroleum-based materials. PU is made from isocyanate functional groups and polyol groups. Diisocyanate and the chain extender form hard segments. Whereas polyol builds soft segments to benefit elastic property of PU/SMPU. Polyols can originate from petroleum as well as renewable materials (e.g. lignocellulosic biomass and vegetable oils). Natural fibres such as CNFs derived from oil palm empty fruit bunch (EFB) is an agricultural waste of palm oil mill, which contains processed rich lignocellulose to produce polyol. Therefore, CNFs can be promoted as a renewable material to produce smart PU. Another renewable material is WF, as an abundant biomass material with low cost, low density and environmental sustainability, which may also be attractive to create smart PU.

Even though the development of smart PU composites for 3D or 4D printing shows good progress, as indicated by various research results for potential applications in biomedical engineering and electronic devices, several challenges still remain concurrently. First of all, printed PU/SMPU composites fabricated by FDM typically generate anisotropic effect on printed parts. Besides, this 3D printing technique also yields printed components with poor accuracy and rough surface finish. These drawbacks may be solved by incorporating post-processing methods (e.g. heat treatment, sanding and polishing). Secondly, material clogging sometimes occurred in FDM. It could be overcome by decreasing the filler content and optimising printing parameters in order to allow the filaments to be ejected through a nozzle tip facilely and deposited onto the build platform layer by layer. The third challenge is related to filler agglomeration in polymer matrix. This issue could be tackled by implementing suitable mixing methods or using additional materials to improve adhesion between fillers and the matrix. Accordingly, it may further enhance filler dispersion level in the matrix. The next challenge is filament buckling caused by low stiffness of the filaments. It may be tackled by increasing the filler content to enhance the elastic modulus of filaments. However, when the filler content is too high, it could give rise to material clogging in the nozzle. The last challenge is that the structures of printed PU/SMPU composites resulting from 3D printing are

commonly categorised as the prototype rather than functional objects due to poor accuracy, rough surface finish, low mechanical strength and other disadvantageous properties. Therefore, it requires some efforts to warrant the quality of printed parts. The hybrid manufacturing methods, post-processing and use of new materials may be necessary to overcome such deficiencies.

3D or 4D printing of smart PU composites has made rapid progress till now. It is indicated by the growing number of studies related to this subject that have been performed by researchers in recent years. Even though most printed PU or SMPU composites are still in prototype form, they show a good potential to become the functional objects in the near future, especially for biomedical engineering and electronic applications. Furthermore, 3D or 4D printing of smart PU composites has a good opportunity to be implemented in garment or textile applications to fabricate smart clothing with the ability to adjust its insulating properties in response to temperature changes where SMPU capability is predominant. The filler inclusion such as nylon in SMPU matrix could enhance the mechanical strength while maintaining the flexibility of resulting composite structures.

Declaration of competing interest

The authors declare that they have no known competing financial interests or personal relationships that could have appeared to influence the work reported in this paper.

Acknowledgements

The first author acknowledged the award of a PhD scholarship supported by the Ministry of Finance of the Republic of Indonesia, Secretariat General of Indonesia Endowment Fund for Education, known as Lembaga Pengelola Dana Pendidikan (LPDP) (Grant number S- 992/LPDP.3/2018).

Appendix A. Supplementary data

Supplementary data to this article can be found online at https://doi.org/10.1016/j.compositesb.2021.109104.

References

[1] Wohler T, Gomet T. Wohlers Report-History of additive manufacturing. Wohler Associates, Inc.; 2014. p. 1–34.
[2] Bogers M, Bilberg A, Hadar R. Additive manufacturing for consumer-centric business models: implications for supply chains in consumer goods manufacturing. Technol Forecast Soc Change 2016;102:225–39. https://doi.org/10.1016/j.techfore.2015.07.024.
[3] Despeisse M, Ford S. The role of additive manufacturing in improving resource efficiency and sustainability. In: IFIP International Conference on Advances, production Management systems. Springer Cham.; 2015. p. 129–36. https://doi.org/10.1007/978-3-319-22759-7_15.
[4] Tumbleston JR, Shirvahyants D, Ermoshkin N, Janusziew R, Johnson AR, Kelly D, et al. Continuous liquid interface production of 3D objects. Science 2015;347:1349–52. https://doi.org/10.1126/science.aaa2397.
[5] Gebhardt A, Hotter J-S, Ziebura D. Impact of SLM build parameters on the surface quality. RTe J 2014;11. https://www.rtejournal.de/ausgabe11/3852.
[6] Wenbin H, Tsui LY, Haiqing G. A study of the staircase effect induced by material shrinkage in rapid prototyping. Rapid Prototyp J 2004;11:82–9. https://doi.org/10.1108/13552540510589449.
[7] Lee AY, An J, Chua CK. Two-way 4D printing: a review on the reversibility of 3D-printed shape memory materials. Engineering 2017;3:663–74. https://doi.org/10.1016/J.ENG.2017.05.014.
[8] Tibbits S, McKnelly C, Olguin C, Dikovsky D, Hirsch S. 4D printing and universal transformation. In: Proceedings of the 34th Annual Conference of the association for computer aided design in Architecture; 2014.
[9] Ge Q, Qi HJ, Dunn ML. Active materials by four-dimension printing. Appl Phys Lett 2013;103:131901. https://doi.org/10.1063/1.4819837.
[10] Pei E. 4D Printing: dawn of an emerging technology cycle. Assemb Autom 2014;34:310–4. https://doi.org/10.1108/AA-07-2014-062.
[11] Howard GT. Biodegradation of polyurethane: a review. Int Biodeterior Biodegrad 2002;49:245–52. https://doi.org/10.1016/S0964-8305(02)00051-3.
[12] Alquichire SA, Valero M. Caster oil polyurethanes as biomaterials. In: Cankaya, editor. Elastomers. Rijeka: Yugoslavia: InTech; 2017. p. 137–57.
[13] Christenson EM, Anderson JM, Hiltner A. Biodegradation mechanisms of polyurethane elastomers. Corrosion Eng Sci Technol 2007;42:312–23. https://doi.org/10.1179/174327807X238909.
[14] Hung KC, Tseng CS, Hsu SH. 3D printing of polyurethane biomaterials. Adv Polyurethane Biomater 2016:149–70. https://doi.org/10.1016/B978-0-08-100614-6.00005-6.
[15] Kausar A. Review on technological significance of photoactive, electroactive, pH sensitive, water-active, and thermo-responsive polyurethane materials. Polym Plast Technol Eng 2017;56:606–16. https://doi.org/10.1080/03602559.2016.1233279.
[16] Seymour RB, Kauffman GB. Polyurethanes: a class of modern versatile materials. J Chem Educ 1992;69:909. https://doi.org/10.1021/ed069p909.
[17] Hung KC, Tseng CS, Dai LG, Hsu SH. Water-based polyurethane 3D printed scaffolds with controlled release function for customized cartilage tissue engineering. Biomaterials 2016;83:156–68. https://doi.org/10.1016/j.biomaterials.2016.01.019.
[18] Feng Z, Li Y, Hao L, Yang Y, Tang T, Tang D, et al. Graphene-reinforced biodegradable resin composites for stereolithographic 3D printing of bone structure scaffolds. Hindawi J Nanomater 2019:9710264. https://doi.org/10.1155/2019/9710264.
[19] Chen Q, Mangadlao JD, Wallat J, Al De Leon, Pokorski JK, Advincula RC. 3D printing biocompatible polyurethane/poly(lactic acid)/graphene oxide nanocomposites: anisotropic properties. ACS Appl Mater Interfaces 2017;9:4015–23. https://doi.org/10.1021/acsami.6b11793.
[20] Jing X, Mi H-Y, Peng X-F, Turng L-S. The morphology, properties, and shape memory behavior of polylactic acid/thermoplastic polyurethane blends. Polym Eng Sci 2014;55:70–80. https://doi.org/10.1002/pen.23873.
[21] Naureen B, Haseeb ASMA, Basirun WJ, Muhamad F. Recent advances in tissue engineering scaffolds based on polyurethane and modified polyurethane. Mater Sci Eng C 2021;118:111228. https://doi.org/10.1016/j.msec.2020.111228.
[22] Feldman D. Polyurethane and polyurethane nanocomposites: recent contributions to medicine. Biointerf Res Appl Chem 2021;11:8179–89. https://doi.org/10.33263/BRIAC111.81798189.
[23] Baqar M, Agag T, Ishida H, Qutubuddin S. Poly(benzoxazine-courethane)s: a new concept for phenolic/urethane copolymers via one-pot method. Polymer 2011;52:307–17. https://doi.org/10.1016/j.polymer.2010.11.052.
[24] Kathalewar M, Joshi P, Sabnis A, Malshe V. Non-isocyanate polyurethanes: from chemistry to applications. RSC Adv 2013;3:4110–29. https://doi.org/10.1039/C2RA21938G.
[25] Mohan D, Sajab MS, Kaco H, Bakarudin SB, Noor AM. 3D printing of UV- curable polyurethane incorporated with surface-grafted nanocellulose. Nanomaterials 2019;9:1–16. https://doi.org/10.3390/nano9121726.
[26] Christ JF, Hohimer CJ, Aliheidari N, Ameli A, Mo C, Potschke P. 3D printing of highly elastic strain sensors using polyurethane/multiwall carbon nonotube composites. In: Sensors and smart structures technologies for Civil, mechanical, and Aerospace systems SPIE. US: O Portland; 2017.
[27] Gupta YN, Bhave TM, Abbas SM, Sharma RB, Setua DK. Low temperature shape memory characteristics of segmented polyurethane-nanoclay composites. J Therm Anal Calorim 2016;124:1449–61. https://doi.org/10.1007/s10973-016-5248-6.
[28] Li W, Jiang X, Wu R, Wang W. Fast shape recovery by changing the grafting ratio in polyurethane/montmorillonite-poly(methyl methacrylate) composites. Polym J 2017;49(2):263–71. https://doi.org/10.1038/pj.2016.98.
[29] Aneja A, Wilkes GL, Rightor EG. Study of slabstock flexible polyurethane foams based on varied toluene diisocyanate isomer ratios. J Polym Sci B Polym Phys 2003;41(3):258–68. https://doi.org/10.1002/polb.10363.
[30] Kim YH, Lee JW, Choi SJ, Han MS, Kim JM, Vim Sb SB, et al. Properties of rigid polyurethane foams blown by HFC-365mfc and distilled water. J Ind Eng Chem 2007;13:1076–82.
[31] Driffield M, Bradley EL, Castle L. A method of test for residual isophorone diisocyanate trimer in new polyester–polyurethane coatings on light metal packaging using liquid chromatography with tandem mass spectrometric detection. J Chromatogr A 2007;1141:61–6. https://doi.org/10.1016/j.chroma.2006.12.005.
[32] Chattopadhyay DK, Raju KVSN. Structural engineering of polyurethane coatings for high performance applications. Prog Polym Sci 2007;32:352–418. https://doi.org/10.1016/j.progpolymsci.2006.05.003.
[33] Courtois J, Baroudi I, Nouvel N, Degrandi E, Pensec S, Ducouret G, et al. Supramolecular soft adhesive materials. Adv Funct Mater 2010;20:1803–11. https://doi.org/10.1002/adfm.200901903.
[34] He Y, Xie D, Zhang X. The structure, microphase-separated morphology, and property of polyurethanes and polyureas. J Mater Sci 2014;49:7339–52. https://doi.org/10.1002/10.1007/s10853-014-8458-y.
[35] Hernandez R, Weksler J, Padsalgikar A, Runt J. In vitro oxidation of high polydimethylsiloxane content biomedical polyurethanes: correlation with the microstructure. J Biomed Mater Res 2008;87:546–56. https://doi.org/10.1002/jbm.a.31823.
[36] Fernandez d'Arlas B B, Rueda L, de la Caba K, Mondragon I, Eceiza A. Microdomain composition and properties differences of biodegradable polyurethanes based on MDI and HDI. Polym Eng Sci 2008;48:519–29. https://doi.org/10.1002/pen.20983.
[37] Jitendra ST, Adekunle TA, Dmitri K. Bio-based nanocomposites: an alternative to traditional composites. J Technol Stud 2009;35:25–32. https://doi.org/10.21061/jots.v35i1.a.4.
[38] Bayer O. Das di-isocyanat-polyadditionsverfahren (polyurethane). Angew Chem 1947;59:257–72. https://doi.org/10.1002/ange.19470590901.

[39] Davis FJ, Mitchell GR. Polymeric materials for rapid manufacturing in rapid manufacturing. In: Bartolo PJ, editor. Stereolithography: materials, processes and applications. Boston: Springer; 2011. p. 113–39. https://doi.org/10.1007/978-0-387-92904-0_5.
[40] Petrovic ZS, Ferguson J. Polyurethane elastomers. Prog Polym Sci 1991;16:695–836. https://doi.org/10.1016/0079-6700(91)90011-9.
[41] Xie F, Huang L, Leng J, Liu Y. Thermoset shape memory polymers and their composites. J Intell Mater Syst Struct 2016;27:2433–55. https://doi.org/10.1177/1045389X16634211.
[42] Gama NV, Ferreira A, Timmons AB. Polyurethane foams: past, present, and future. Materials 2018;11:1841–51. https://doi.org/10.1177/10.3390/ma11101841.
[43] Khatoon H, Ahmad S. A review on conducting polymer reinforced polyurethane composites. J Ind Eng Chem 2017;53:1–22. https://doi.org/10.1016/j.jiec.2017.03.036.
[44] Diamant RME. Thermal and Acoustic insulation. Amsterdam, The Netherlands: Butterworth-Heinemann; 1986. p. 376.
[45] Davim JP. The design and manufacture of medical devices. Cambridge, UK: Woodhead Publishing Ltd; 2012. p. 386.
[46] Chen T. Compound yarns. In: Gong RH, editor. Specialist Yarn and Fabrict structures development and applications. Woodhead Publishing Series in Textiles; 2011. p. 1–20.
[47] Chegolya AS, Radushkevich BV. Polyurethane fibres, properties, processing, and application. Fibre Chem 1982;13:292–8. https://doi.org/10.1007/BF00548220.
[48] Puppi D, Chiellini F. Biodegradable polymers for biomedical additive manufacturing. Appl Mater Today 2020;20:100700. https://doi.org/10.1016/j.apmt.2020.100700.
[49] Joseph J, Patel RM, Wenham A, Smith J. Biomedical applications of polyurethane materials and coatings. Trans Inst Met Finish 2018;96:121–9. https://doi.org/10.1080/00202967.2018.1450209.
[50] Guelcher SA. Biodegradable polyurethanes: synthesis and applications in regenerative medicine. Tissue Eng B 2008;14:3–17. https://doi.org/10.1089/teb.2007.0133.
[51] Tatai L, Moore TG, Adhikari R, Malherbe F, Jayasekara R, Griffiths I, Gunatillake PA. Thermoplastic biodegradable polyurethanes: the effect of chain extender structure on properties and in-vitro degradation. Biomaterials 2007;28:5407–17. https://doi.org/10.1016/j.biomaterials.2007.08.035.
[52] Anastas PT, Warner JC. Green chemistry: theory and Practice. New York: Oxford University Press; 1998.
[53] Tenorio- Alfonso A, Sanchez MC, Franco JM. A review of the sustainable approaches in the production of bio- based polyurethanes and their applications in the adhesive field. J Polym Environ 2020;28:1–26. https://doi.org/10.1007/s10924-020-01659-1.
[54] Octave S, Thomas D. Biorefinery: toward an industrial metabolism. Biochimie 2009;91:659–64. https://doi.org/10.1016/j.biochi.2009.03.015.
[55] Isikgor FH, Becer CR. Lignocellulosic biomass: a sustainable platform for the production of bio-based chemicals and polymers. Polym Chem 2015;6:4497–559. https://doi.org/10.1039/C5PY00263J.
[56] Jeong H, Park J, Kim S, Lee J, Ahn N, Roh H. Preparation and characterization of thermoplastic polyurethanes using partially acetylated kraft lignin. Fibers Polym 2013;14:1082–93. https://doi.org/10.1007/s12221-013-1082-7.
[57] Grifni G, Passoni V, Suriano R, Levi M, Turri S. Polyurethane coatings based on chemically unmodifed fractionated lignin. ACS Sustainable Chem Eng 2015;3:1145–54. https://doi.org/10.1021/acssuschemeng.5b00073.
[58] Tzounis L, Petousis M, Grammatikos S, Vidakis N. 3D printed thermoelectric polyurethane/multiwalled carbon nanotube nanocomposites: a novel approach towards the fabrication of flexible and stretchable organic thermoelectrics. Materials 2020;13:2879. https://doi.org/10.3390/ma13122879.
[59] Gama N, Ferreira A, Timmons AB. 3D printed cork/polyurethane composite foams. Mater Des 2019;179:107905. https://doi.org/10.1016/j.matdes.2019.107905.
[60] Lathers S, La Belle J. Additive manufactured biomimicking actuator with shape memory polymer composite for prosthetic actuators. 3D Print Addit Manuf 2017;4:201–13. https://doi.org/10.1089/3dp.2017.0048.
[61] Evans KA, Kennedy ZC, Arey BW, Christ JF, Schaef HT, Nune SK, et al. Chemically active, porous 3D-printed thermoplastic composites. ACS Appl Mater Interfaces 2018;10:15112–21. https://doi.org/10.1021/acsami.7b17565.
[62] Xiang D, Zhang X, Li Y, Jones EH, Zheng Y, Wang L, et al. Enhanced performance of 3D printed highly elastic strain sensors of carbon nanotube/thermoplastic polyurethane nanocomposites via non-covalent interactions. Compos B Eng 2019;176:107250. https://doi.org/10.1016/j.compositesb.2019.107250.
[63] Bi H, Ren Z, Guo R, Xu M, Song Y. Fabrication of flexible wood flour/thermoplastic polyurethane elastomer composites using fused deposition molding. Ind Crop Prod 2018;122:76–84. https://doi.org/10.1016/j.indcrop.2018.05.059.
[64] Liu J, Li W, Guo Y, Zhang H, Zhang Z. Improved thermal conductivity of thermoplastic polyurethane via aligned boron nitride platelets assisted by 3D printing. Compos Part A 2019;120:140–6. https://doi.org/10.1016/j.compositesa.2019.02.026.
[65] Kim M, Jung J, Jung S, Moon YH, Kim D-H, Kim JH. Piezoresistive behaviour of additively manufactured multi-walled carbon nanotube/thermoplastic polyurethane nanocomposites. Materials 2019;12:2613. https://doi.org/10.3390/ma12162613.
[66] Leng J, Wu J, Zhang J. Preparation of thermoplastic polyurethane parts reinforced with in situ polylactic acid microfibers during fused deposition modeling: the influences of deposition-induced effects. ACS Ind. Eng. Chem. Res. 2019;58:21476–84. https://doi.org/10.1021/acs.iecr.9b04285.
[67] Xiang D, Zhang X, Jones EH, Zhu W, Zhou Z, Shen Y, et al. Synergistic effects of hybrid conductive nanofillers on the performance of 3D printed highly elastic strain sensors. Compos Appl Sci Manuf 2020;129:105730. https://doi.org/10.1016/j.compositesa.2019.105730.
[68] Li Z, Wang Z, Gan X, Fu D, Fei G, Xia H. In: Selective laser sintering 3D printing: a way to Construct 3D electrically conductive segregated network in polymer matrix. Macromolecular Materials and Engineering; 2017. p. 1700211. https://doi.org/10.1002/mame.201700211.
[69] Gan X, Wang J, Wang Z, Zheng Z, Lavorgna M, Ronca A, et al. Simultaneous realization of conductive segregation network microstructure and minimal surface porous macrostructure by SLS 3D printing. Mater Des 2019;178:107874. https://doi.org/10.1016/j.matdes.2019.107874.
[70] Joo H, Cho S. Comparative studies on polyurethane composites filled with polyaniline and graphene for DLP-type 3D printing. Polymers 2020;12:1–11. https://doi.org/10.3390/polym12010067.
[71] Ibrahim F, Mohan D, Sajab MS, Bakarudin SB, Kaco H. Evaluation of the compatibility of organosolv lignin-graphene nanoplatelets with photo-curable polyurethane in stereolithography 3D printing. Polymers 2019;11:1544. https://doi.org/10.3390/polym11101544.
[72] Jain PK, Senthilkumaran K, Pandey PM, Rao PVM. Advances in materials for powder based rapid prototyping. In: International Conference on recent Advances in materials and processing. Coimbatore, India: PSG-tech; 2006.
[73] Jiang P, Ji Z, Zhang X, Liu Z, Wang X. Recent advances in direct ink writing of electronic components and functional devices. Progr Addit Manuf 2018;3:65–86.
[74] Herzberger J, Sirrine JM, Williams CB, Long TE. Polymer design for 3D printing elastomers: recent advances in structure, properties, and printing. Prog Polym Sci 2019;97:101144.
[75] Stansbury JW, Idacavage MJ. 3D printing with polymers: challenges among expanding options and opportunities. Dent Mater 2016;32:54–64. https://doi.org/10.1016/j.dental.2015.09.018.
[76] Stampfl J, Baudis S, Heller C, Liska R, Neumeister A, Kling R, et al. Photopolymers with tunable mechanical properties processed by laser-based high- resolution stereolithography. J Micromech Microeng 2008;18:125014. https://doi.org/10.1088/0960-1317/18/12/125014.
[77] Armington AF. Standard purification techniques. Ann N Y Acad Sci 2006;118:613–7. https://doi.org/10.3390/ma13010211.
[78] Gibson I, Rosen DW, Stucker B. Additive manufacturing technologies. New York: Springer; 2010.
[79] Eom A-H, Won J-P. Selection of functional materials for surface-coating of structural synthetic fibres and development of a 3D-printing system for their manufacture. Compos Struct 2020;249:112567. https://doi.org/10.1016/j.compstruct.2020.112567.
[80] Su J-W, Gao W, Trinh K, Kenderes SM, Pulatsu ET, Zhang C, et al. 4D printing of polyurethane paint-based composites. Int J Soc Netw Min 2019;10:237–48. https://doi.org/10.1080/19475411.2019.1618409.
[81] Yuan S, Li S, Zhu J, Tang Y. Additive manufacturing of polymeric composites from material processing to structural design. Composites Part B 2021;219:108903. https://doi.org/10.1016/j.compositesb.2021.108903.
[82] Wang Y, Li X. 4D-printed bi-material composite laminate for manufacturing reversible shape-change structures. Composites Part B 2021;219:108918. https://doi.org/10.1016/j.compositesb.2021.108918.
[83] Legeza O, Roder J, Hess BA. QC-DMRG study of the ionic-neutral curve crossing of LiF. Mol Phys 2009;101:2019–28.
[84] Lin D, Nian Q, Deng B, Jin S, Hu Y, Wang W, et al. Three-dimensional printing of complex structures:man made or toward nature? ACS Nano 2014;8:9710–5. https://doi.org/10.1021/nn504894j.
[85] Stepashkin AA, Chukov DI, Senatov FS, Salimon AI, Korsunsky AM, Kaloshkin SD. 3D-printed PEEK-carbon fiber (CF) composites: structure and thermal properties. Compos Sci Technol 2018;164:319–26. https://doi.org/10.1016/j.compscitech.2018.05.032.
[86] Gil L. New cork-based materials and applications. Materials 2015;8:625–37. https://doi.org/10.3390/ma8020625.
[87] Daver F, Lee KPM, Brandt M, Shanks R. Cork–PLA composite filaments for fused deposition modelling. Compos Sci Technol 2018;168:230–7. https://doi.org/10.1016/j.compscitech.2018.10.008.
[88] Brites F, Malca C, Gaspar F, Horta JF, Franco MC, Biscaia S, et al. Cork plastic composite optimization for 3D printing applications. Procedia Manuf 2017;12:156–65. https://doi.org/10.1016/j.promfg.2017.08.020.
[89] Shi X, Chen B, Tuo X, Gong Y, Guo J. Study on performance characteristics of fused deposition modeling 3D-printed composites by blending and lamination. J Appl Polym Sci 2020:1–7. https://doi.org/10.1002/app.49926. e32495.
[90] Tao Y, Shao J, Li P, Shi SQ. Application of a thermoplastic polyurethane/polylactic acid composite filament for 3D-printed personalized orthosis. Mater Tehnol 2019;53:71–6. https://doi.org/10.17222/mit.2018.180.
[91] Lamaming J, Hashim R, Sulaiman O, Leh CP, Sugimoto T, Nordin NA. Cellulose nanocrystals isolated from oil palm trunk. Carbohydr Polym 2015;127:202–8. https://doi.org/10.1016/j.carbpol.2015.03.043.
[92] Chan CH, Chia C-H, Zakaria S, Sajab MS, Chin SX. Cellulose nanofibrils: a rapid adsorbent for the removal of methylene blue. RSC Adv 2015;5:18204–12. https://doi.org/10.1016/10.1039/C4RA15754K.
[93] Sajab MS, Chia CH, Chan CH, Zakaria S, Kaco H, Chook SW, et al. Bifunctional graphene oxide-cellulose nanofibril aerogel loaded with Fe(III) for the removal of cationic dye via simultaneous adsorption and Fenton oxidation. RSC Adv 2016;6:19819–25. https://doi.org/10.1039/C5RA26193G.

[94] Hou M, Xu M, Li B. Enhanced electrical conductivity of cellulose nanofiber/graphene composite paper with a sandwich structure. ACS Sustainable Chem Eng 2018;6:2983–90. https://doi.org/10.1021/acssuschemeng.7b02683.

[95] Rahmani H, Najafi SHM, Matin SS, Ashori A. Mechanical properties of carbon fiber/epoxy composites: effects of number of plies, fiber contents, and angle-ply layers. Polym Eng Sci 2013;54:2676–82. https://doi.org/10.1002/pen.23820.

[96] Parizi MT, Ebrahimi GR, Ezatpour HR. Effect of graphene nanoplatelets content on the microstructural and mechanical properties of AZ80 magnesium alloy. Mater Sci Eng 2019;742:373–89. https://doi.org/10.1016/j.msea.2018.11.025.

[97] Park YT, Qian Y, Chan C, Suh T, Nejhad MG, Macosko CW, et al. Epoxy toughening with low graphene loading. Adv Funct Mater 2015;25:575–85. https://doi.org/10.1002/adfm.201402553.

[98] Qu P, Gao Y, Wu G-F, Zhang L-P. Nanocomposites of poly(lactic acid) reinforced with cellulose nanofibrils. Bioresources 2010;5:1811–23.

[99] Yang Z, Li X, Si J, Cui Z, Peng K. Morphological, mechanical and thermal properties of poly (lactic acid) (PLA)/cellulose nanofibrils (CNF) composites nanofiber for tissue engineering. J Wuhan Univ Technol Mater Sci 2019;34:207–15. https://doi.org/10.1007/s11595-019-2037-7.

[100] Zainuddin MF, Raikhan NN, Othman NH, Abdullah WFH. Synthesis of reduced graphene oxide (rGO) using different treatments of graphene oxide (GO). In: 3rd International Conference on Global sustainability and chemical engineering (ICGSCE). Bristol, UK, Putrajaya, Malaysia: IOP Publishing; 2018. p. 358. https://doi.org/10.1088/1757-899X/358/1/012046.

[101] Venkatesh A, Thunberg J, Moberg T, Klingberg M, Hammar L, Peterson A, et al. Cellulose nanofibril-reinforced composites using aqueous dispersed ethylene-acrylic acid copolymer. Cellulose 2018;25:4577–89. https://doi.org/10.1007/s10570- 018-1875-3.

[102] Jang J. Conducting polymer nanomaterials and their applications. Adv Polym Sci 2006;199:189–259. https://doi.org/10.1007/12_075.

[103] Park H, Kim T, Huh J, Kang M, Lee J, Yoon H. Anisotropic growth control of polyaniline nanostructures and their morphology-dependent electrochemical characteristics. ACS Nano 2012;6:7624–33. https://doi.org/10.1021/nn3033425.

[104] Demir MM, Menceloglu YZ, Erman B. Aggregation of fillers blended into random elastomeric networks: theory and comparison with experiments. Macromol Chem Phys 2006;207:1515–24. https://doi.org/10.1002/macp.200600185.

[105] Chen C-H, Kan Y-T, Mao C-F, Liao W-T, Hsieh C-D. Fabrication and characterization of water-based polyurethane/polyaniline conducting blend films. Surf Coating Technol 2013;231:71–6. https://doi.org/10.1016/j.surfcoat.2012.03.056.

[106] Song B, Tuan C, Li L, Zhu Y, Moon K, Wong CP. Highly conductive polyurethane/polyaniline-based composites for wearable electronic applications. In: The 2016 IEEE 66th electronic components and technology Conference (ECTC). NV, USA: Las Vegas; 2016. https://doi.org/10.1109/ECTC.2016.54.

[107] Hong SY, Oh JH, Park H, Yun JY, Jin SW, Sun L, et al. Polyurethane foam coated with a multi-walled carbon nanotube/polyaniline nanocomposite for a skin- like stretchable array of multi-functional sensors. NPG Asia Mater 2017;9:e448. https://doi.org/10.1038/am.2017.194.

[108] Alves P, Coelho JFJ, Haack J. Surface modification and characterization of thermoplastic polyurethane. Eur Polym J 2009;45:1412–9. https://doi.org/10.1016/j.eurpolymj.2009.02.011.

[109] Li QY, Wu HJ, Lu CH. Modification of POE-g-MAH for w-PDM/LLDPE blends. J Chin Plast Ind 2015;43:28–31.

[110] Wang X, Luo X, Wang X. Study on blends of thermoplastic polyurethane and aliphatic polyester: morphology, rheology, and properties as moisture vapor permeable films. Polym Test 2005;24:18–24. https://doi.org/10.1016/j.polymertesting.2004.08.003.

[111] Jaisankar SN, Radhakrishnan G. Effect of compatibilizer on morphology and mechanical properties of TPU/SAN blends. Polym Eng Sci 2000;40:621–6. https://doi.org/10.1002/pen.11192.

[112] Adsuar MSS, Solano AL, Amorós DC, Rueda LI. Influence of the nature and the content of carbon fiber on properties of thermoplastic polyurethane-carbon fiber composites. J Appl Polym Sci 2003;90:2676–83. https://doi.org/10.1002/app.12916.

[113] Vajrasthira C, Amornsakchai T, Limcharoen SB. Fiber-matrix interactions in aramid-short-fiber-reinforced thermoplastic polyurethane composites. J Appl Polym Sci 2003;87:1059–67. https://doi.org/10.1002/app.11484.

[114] Yao X, Qi X, He Y, Tan D, Chen F, Fu Q. Simultaneous reinforcing and toughening of polyurethane via grafting on the surface of microfibrillated cellulose. J ACS Appl Mater Interfaces 2014;6:2497–507. https://doi.org/10.1021/am4056694.

[115] Chen Q, Xiang D, Wang L, Tang Y, Harkin-Jones E, Zhao C, et al. Facile fabrication and performance of robust polymer/carbon nanotube coated spandex fibers for strain sensing. Compos Appl Sci Manuf 2018;112:186–96. https://doi.org/10.1016/j.compositesa.2018.06.009.

[116] Lin L, Liu S, Zhang Q, Li X, Ji M, Deng H, et al. Towards tunable sensitivity of electrical property to strain for conductive polymer composites based on thermoplastic elastomer. ACS Appl Mater Interfaces 2013;5:5815–24. https://doi.org/10.1021/am401402x.

[117] Schmid M, Amando A, Wegener K. Materials perspective of polymers for additive manufacturing with selective laser sintering. J Mater Res 2014;29:1824–32. https://doi.org/10.1557/jmr.2014.138.

[118] Childs THC, Tontowi AE. Selective laser sintering of a crystalline and a glass-filled crystalline polymer: experiments and simulations. Proc Inst Mech Eng, Part B 2001;215:1481–95. https://doi.org/10.1243/0954405011519330.

[119] Frenkel J. Viscous flow of crystalline bodies under the action of surface tension. J Phys 1945;9:385–91.

[120] Tibbits S. The emergence of 4D printing. In: TED Talks; 2013.

[121] Mitchell A, Lafont U, Hołyńska M, Semprimoschnig C. Additive manufacturing- A review of 4D printing and future applications. Addit Manuf 2018;24:606–26. https://doi.org/10.1016/j.addma.2018.10.038.

[122] Momeni F, Hasani SM, Liu X, Ni J. A review of 4D printing. Mater Des 2017;122:42–79. https://doi.org/10.1016/J.MATDES.2017.02.068.

[123] Sun L, Huang WM. Mechanisms of the multi-shape memory effect and temperature memory effect in shape memory polymers. Soft Matter 2010;6:4403–6. https://doi.org/10.1039/C0SM00236D.

[124] Sun L, Huang WM, Ding Z, Zhao Y, Wang CC, Purnawali H, et al. Stimulus responsive shape memory materials: a review. Mater Des 2012;33:577–640. https://doi.org/10.1016/j.matdes.2011.04.065.

[125] Ly ST, Kim JY. 4D printing – fused deposition modeling printing with thermal-responsive shape memory polymers. Int J Precis Eng Manuf Green Technol 2017;4:267–72. https://doi.org/10.1007/s40684-017-0032-z.

[126] Rosales CAG, Duarte MFG, Kim H, Chavez L, Hodges D, Mandal P, et al. 3D printing of Shape Memory Polymer (SMP)/Carbon Black (CB) nanocomposites with electro-responsive toughness enhancement. Mater Res Express 2018;5:1–14. https://doi.org/10.1088/2053-1591/AACD53.

[127] Bi H, Ye G, Yang H, Sun H, Ren Z, Guo R, et al. Near infrared-induced shape memory polymer composites with dopamine modified multiwall carbon nanotubes via 3D-printing. Eur Polym J 2020;136:109920. https://doi.org/10.1016/j.eurpolymj.2020.109920.

[128] Bi H, Xu M, Ye G, Guo R, Cai L, Ren Z. Mechanical, thermal, and shape memory properties of three-dimensional printing biomass composites. Polymers 2018;10:1234. https://doi.org/10.3390/polym10111234.

[129] Kashyap D, Kumar PK, Kanagaraj S. 4D printed porous radiopaque shape memory polyurethane for endovascular embolization. Addit Manuf 2018;24:687–95. https://doi.org/10.1016/j.addma.2018.04.009.

[130] Kabir S, Lee S. Study of shape memory and tensile property of 3D printed sinusoidal sample/nylon composite focused on various thicknesses and shape memory cycles. Polymers 2020;12:1600. https://doi.org/10.3390/polym12071600.

[131] MatWeb L. MatWeb - material property data. 2020. http://www.matweb.com/search/QuickText.aspx. [Accessed 8 October 2020].

[132] Christ JF, Aliheidari N, Ameli A, Potschke P. 3D printed highly elastic strain sensors of multiwalled carbon nanotube/thermoplastic polyurethane nanocomposites. Mater Des 2017;131:394–401. https://doi.org/10.1016/j.matdes.2017.06.011.

[133] Strek T, Jopek H, Wojciechowski KW. The influence of large deformations on mechanical properties of sinusoidal ligament structures. Smart Mater Struct 2016;25:054002. https://doi.org/10.1088/0964-1726/25/5/054002.

[134] Wu W, Ye W, Wu Z, Geng P, Wang Y, Zhao J. Influence of layer thickness, raster angle, deformation temperature and recovery temperature on the shape- memory effect of 3D-printed polylactic acid samples. Materials 2017;10:1–16. https://doi.org/10.3390/ma10080970.

[135] Nejad HB, Baker RM, Mather PT. Preparation and characterization of triple shape memory composite foams. Soft Matter 2014;10:8066–74. https://doi.org/10.1039/C4SM01379D.

[136] Feng X, Zhang G, Zhuo S, Jiang H, Shi J, Li F, et al. Dual responsive shape memory polymer/clay nanocomposites. Compos Sci Technol 2016;129:53–60. https://doi.org/10.1016/j.compscitech.2016.04.008.

[137] Jing X, Mi HY, Huang HX, Turng LS. Shape memory thermoplastic polyurethane (TPU)/poly (ε-caprolactone) (PCL) blends as self-knotting sutures. J Mechan Behav Biomed Mater 2016;64:94–103. https://doi.org/10.1016/j.jmbbm.2016.07.023.

[138] Lu C, Liu Y, Liu X, Wang C, Wang J, Chu F. Sustainable multiple- and multi stimulus-shape-memory and self-healing elastomers with semi- interpenetrating network derived from biomass via bulk radical polymerization. ACS Sustainable Chem Eng 2018;6:6527–35. https://doi.org/10.1021/acssuschemeng.8b00329.

[139] Mosleh Y, Ebrahimi NG, Mahdavian A, Ashjari M. TPU/PCL/nanomagnetite ternary shape memory composites: studies on their thermal, dynamic-mechanical, rheological and electrical properties. Iran Polym J (Engl Ed) 2014;23:137–45. https://doi.org/10.1007/s13726-013-0209-4.

[140] Gupta A, Maharjan A, Kim BS. Shape memory polyurethane and its composites for various applications. Appl Sci 2019;9:1–29. https://doi.org/10.3390/app9214694.

[141] Liu C, Qin H, Mather PT. Review of progress in shape-memory polymers. J Mater Chem 2007;17:1543–58. https://doi.org/10.1039/B615954K.

[142] Yang Q, Zheng W, Zhao W, Peng C, Ren J, Yu Q, et al. One-way and two-way shape memory effects of a high-strain cis-1,4-polybutadiene–polyethylene copolymer based dynamic network via self-complementary quadruple hydrogen bonding. Polym Chem 2019;10:718–26. https://doi.org/10.1039/C8PY01614C.

[143] Ware T, Hearon K, Lonnecker A, Wooley KL, Maitland DJ, Voit W. Triple- shape memory polymers based on self-complementary hydrogen bonding. Macromelecules 2012;45:1062–9. https://doi.org/10.1021/ma202098s.

[144] Xian J, Geng J, Wang Y, Xia L. Quadruple-shape-memory effect of TPI/LDPE/HDPE composites. Polym Adv Technol 2018;29:982–8. https://doi.org/10.1002/pat.4209.

[145] Guerado E, Caso E. Challenges of bone tissue engineering in orthopaedic patients. World J Orthoped 2017;8:87–98. https://doi.org/10.5312/wjo.v8.i2.87.

[146] Zhang Y, Hu J, Zhao X, Xie R, Qin T, Ji F. Mechanically robust shape memory polyurethane nanocomposites for minimally invasive bone repair. ACS Appl Bio Mater 2019;2:1056–65. https://doi.org/10.1021/acsabm.8b00655.

[147] Chandler RF, Clauser CE, McMconville JT, Reynolds HM, Young JW. Investigation of inertial properties of the human hand. Washington, DC: U.S. Department of Transportation; 1957.

[148] Tozeren A. Human body Dynamics: Classical mechanic and human movement. New York: Springer-Verlag; 2000.
[149] Macdonald E, Salas R, Espalin D, Perez M, Aguilera E, Muse D, et al. 3D printing for the rapid prototyping of structural electronics. IEEE Access 2014;2:234–42. https://doi.org/10.1109/ACCESS.2014.2311810.
[150] Tzounis L, Gravalidis C, Vassiliadou S, Logothetidis S. Fiber yarns/CNT hierarchical structures as thermoelectric generators. Mater Today: Proc 2017;4:7070–5. https://doi.org/10.1016/j.matpr.2017.07.040.